Universidad del Desarrollo
Facultad de Gobierno
Centro de Investigación en Complejidad Social

NEUROBIOLOGICAL CODING OF VALUE AND PREDICTION ERROR IN STABLE AND VOLATILITY UNCERTAINTY CONTEXTS IN HUMAN DECISION-MAKING

BY: GABRIELA VALDEBENITO OYARZO

Thesis submitted to the Faculty of Government of the Universidad Del Desarrollo for the academic degree of Doctor in Sciences of Social Complexity

SUPERVISOR THESIS:

Sr. PABLO BILLEKE BOBADILLA

July, 2022

SANTIAGO, CHILE

Declaration of Authorship

© I authorize to publish this thesis online after January 2022.

I declare that this thesis titled, "*NEUROBIOLOGICAL CODING OF VALUE AND PREDICTION ERROR IN STABLE AND VOLATILITY UNCERTAINTY CONTEXTS IN HUMAN DECISION-MAKING*" and the work presented in it are my own. I confirm that:

- This work was done wholly or mainly while in candidature for a research degree at this University.
- Where any part of this thesis has previously been submitted for a degree or any other qualification at this University or any other institution, this has been clearly stated.
- Where I have consulted the published work of others, this is always clearly attributed.
- Where I have quoted from the work of others, the source is always given. With the exception of such quotations, this thesis is entirely my own work.
- I have acknowledged all main sources of help.
- Where the thesis is based on work done by myself jointly with others, I have made clear exactly what was done by others and what I have contributed myself.

Dedication

Dedicated to my mother Patricia, my father Juan Fernando, my sister Romina, my niece Leonor and to the memory of my grandfather Camilo.

Acknowledgments

- To my professor Pablo Billeke Bobadilla.
- To the project Fondecyt de Iniciación nro 11140535 and Fondecyt regular nro 1181295 for sponsoring the realization of this work.
- To the neuroscience division of the Center for Research in Social Complexity (neuroCICS) for facilitating the completion of this work.
- To my fellow PhD students.
- To the more than 100 participants who contributed to this research and with that to the generation of scientific knowledge.
- To my family and friends for their support.

Resumen

Los neurocientíficos que estudian el proceso de toma de decisiones económicas se han centrado en investigar cómo los seres humanos, y otras especies animales, eligen entre diferentes opciones guiadas por refuerzo. El cálculo de la probabilidad de obtener una recompensa y el valor de las opciones disponibles son elementos que deben ser estimados con precisión para obtener buenos resultados. Sin embargo, en el contexto de la vida cotidiana, este proceso puede tener diferentes grados de complejidad dependiente del nivel de información que poseamos desde las experiencias previas y que nos entrega el ambiente.

La estimación de los factores que afectan una elección implica un proceso de aprendizaje que está mediado por la capacidad de diseñar y actualizar un modelo interno del valor de las probabilidades de las opciones a través de la detección de la magnitud del error de la predicción.

Se han investigado extensamente los mecanismos neurobiológicos que subyacen al proceso de toma de decisiones en diferentes contextos de incertidumbre. Para la condición de ambigüedad se ha observado la presencia de actividad en la corteza parietal cuyo rol aún no está claro y es el centro de esta investigación.

En la presente tesis se presenta el estudio de la toma de decisiones en diferentes contextos de incertidumbre (estable y volátil) para evaluar los mecanismos neurobiológicos de la computación de la incertidumbre. Para esta investigación se han diseñado dos tareas experimentales con diferentes condiciones que afectan directamente al grado de información que reciben los jugadores para hacer una predicción. Las hipótesis que se evalúan en esta investigación son: (i) La corteza parietal contribuye causalmente en la valorización de la información ambigua durante la toma de decisiones en contextos de incertidumbre estable. (ii) La corteza parietal participa en la detección del cambio de las contingencias en contexto de incertidumbre volátil.

Para testear nuestras hipótesis se realizaron dos experimentos:

1. Sesenta y seis participantes resolvieron una tarea de toma de decisiones probabilísticas (PDM) en dos sesiones experimentales. En primera instancia, los sujetos realizaron el experimento bajo resonancia magnética funcional para medir los cambios de la señal BOLD. Nuestro

análisis se centró en observar la actividad neurobiológica y conductual asociada a la construcción del valor de las probabilidades en contexto de ambigüedad. Los resultados mostraron una importante activación de la corteza parietal posterior y el surco intra parietal, también se observó actividad en el giro frontal inferior asociado al valor absoluto del error en la predicción. En concordancia con el objetivo de evaluar nuestra hipótesis, en una segunda sesión experimental, los participantes realizaron la misma tarea bajo la medición de la actividad electrifisiológica y la estimulación inhibitoria previo al feedback en los dos focos de la corteza parietal para perturbar el procesamiento cognitivo y conductual de la probabilidad. Los resultados revelaron que la estimulación de la corteza parietal afectó la construcción de la probabilidad ambigua. Además, se observó una disminución en la actividad theta de la corteza frontal inferior asociado al error en la predicción demostrando un rol causal de la corteza parietal en la computación de la ambigüedad.

2. Treinta participantes resolvieron una tarea de toma de decisiones en contexto de incertidumbre estable y volátil (DMUV). La actividad cerebral fue medida bajo resonancia magnética funcional. Los análisis se centraron en calcular el valor de la función de aprendizaje en cada contexto del experimento y la actividad neurobiológica durante el periodo del feedback. Los resultados mostraron un aumento de la señal BOLD en la corteza parietal asociado a la función de aprendizaje en el contexto de alta incertidumbre volátil.

Contents

List of Figures

List of Tables

Chapter 1

Introduction

Making a decision is the act of choosing an option among two or more possibilities to obtain an expected result, this process is performed constantly in everyday life from simple decisions such as choosing what to eat or complex decisions such as defining a life plan, so deciding is not a trivial process in the life of the human being.

The process of making a decision involves making a prediction of what we estimate will happen if we choose an option among the available variety, so this process always involves a degree of uncertainty that affects it. Neuroscientists have defined five steps that the brain computes during the decision-making process: *(i)* The representation, alludes to the initial part of the process where the course of action to resolve a situation is planned according to the internal and external state, *(ii)* evaluation of the available options to choose from which can be through the Pavlovian system, the habit system or the goal-directed system. *(iii)* the action of selecting one of the available options based on the appraisal, *(iv)* the evaluation of the outcome of the decision taken and *(v)* the learning to be used in similar situations in the future and that will directly affect the appraisal process (Quirk & Mueller, 2008; Kahneman & Tversky, 2013).

We can usually face two types of decisions. Perceptual decisions that are determined by states of the world, e.g., oranges are bigger than lemons. Value-based decisions are determined by

subjective preferences of individuals, e.g., oranges are tastier than lemons (Polanía, Krajbich, Grueschow, & Ruff, 2014), in this research we focus on this type of decision. Current models of value-based decision making consider choices as a two-stage process, ranging from the " valuation" of each option under consideration to the "selection" of the best option based on their subjective values (Domenech, Redouté, Koechlin, & Dreher, 2018).

Decision making is a process that occurs in the animal species and in humans, in this sense we use tools from economics that provides decision paradigms and their variables, psychology that through data allows us to understand the behavior and neurobiology contributes by elucidating the neural events that underlie the decision making process (Rangel, Camerer, & Montague, 2008).

1.1 Varieties of uncertainty in decision-making

Deciding involves choosing between two or more options to obtain the best possible expected outcome, so uncertainty is something that characterizes this process. Uncertainty arises in a situation where the degree of information is limited (Huettel, Song, & McCarthy, 2005), and is defined as a probabilistic model where the decision maker is partially or completely unaware of the state of nature of the world where he/she decides, therefore, the individual is unable to predict precisely which option should be chosen to obtain the best expected outcome. In this context, we can encounter two levels of uncertainty:

- Risk: First-order uncertainty. There is much discussion about the meaning of this condition, e.g., clinically it is the probability of obtaining a negative outcome (e.g., health risks in obese patients). Economists such as von Neumann and Knight have defined risk as the decision-making condition where the probability distribution is known but the outcome is uncertain. Assuming a situation where the probability distribution has a normal Gaussian

distribution, the standard deviation can be higher or lower leading to a higher or lower risk state (see Figure 1.1).

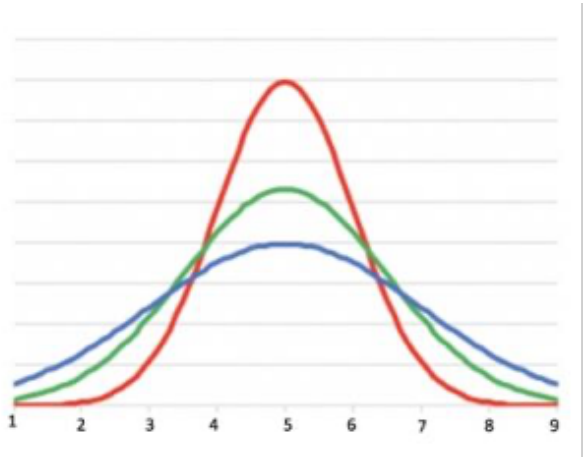

Figure 1.1: **Representation of different contexts of probability distribution**, where: Risk < Risk' < Risk"

- Ambiguity: Second-order uncertainty characterized by the lack of knowledge of the distribution of the probabilities of the options, therefore, neither the arithmetic mean nor the standard deviation that characterizes the probabilistic distribution is known (Glimcher & Fehr, 2013).

As for the context of decision making under uncertainty, the factors that modulate each condition may remain stable or change over time. Here I present two contexts of decision making under uncertainty:

- Stable uncertainty: Uncertainty context of a decision-making task where the factors characterizing the condition remain stable over time, i.e. the mean and standard deviation (or dispersion) of the data do not vary during the course of the task.

- Volatility: Uncertainty context of a decision making task where the factors that characterize the condition undergo changes over time. Factor changes can be:

    1. Change in the mean of the data, the standard deviation remains stable.
    2. Change in the standard deviation of the data, the mean remains stable.
    3. Change in the standard deviation and mean of the data.

Detecting, processing and resolving uncertainty adequately is a key element in making correct decisions, so the success of decisions depends on the ability to form a stable representation of the association of a specific stimulus (S) with a response (R) linked to a positive or negative outcome(O) (S-R-O) (Sutton & Barto, 2018).

Three distinct forms of uncertainty can be identified: *(1)* Expected uncertainty: S-R-O rules learned from past events are weak predictors of the outcomes of future actions, and this unreliability is known and stable. *(2)* Unexpected uncertainty: an infrequent fundamental change in the environment that invalidates existing S-R-O rules, which are no longer capable of accurately predicting the outcomes of our actions. *(3)* Volatility: frequent changes in the environment that require constant updating of the S-R-O rules (Bland et al., 2012)

1.2 Probabilistic brain computation

The brain is an organ capable of processing information from the external and internal world, stimuli are captured by the senses allowing the brain to process the information. Studies suggest that the human mind represents data in the form of a probabilistic distribution (Knill & Pouget, 2004; Clark, 2013; Ma & Jazayeri, 2014). For example, there are multiple factors that can alter the sensory perception of the stimuli we receive from the outside world, so the brain must be able to handle uncertainty to guide the correct course of our actions, which Helmholtz (1860/1962)

called unconscious probabilistic inference, indicating that the brain naturally constructs probability distributions in information processing.

In the context of decision making under uncertainty, especially when there is a high degree of uncertainty, it is necessary to make mental inferences of how we estimate the world to work in order to make an initial prediction of the outcomes that may be obtained by choosing an option. Inference of future outcomes that guide decision making requires knowledge of the associative structure of the environment, the so-called cognitive map that allows us to mentally simulate the likely consequences of cognitive decisions. Inference-based behaviour has two processes: *(1)*, which uses knowledge about the associative structure of the world to infer outcomes when direct experience is lacking; *(2)*, which infers the present value of options when the desirability of the associated outcome has changed since the original learning experience.

More recent studies are based on the notion of a Bayesian brain, where a probabilistic model of the world is constructed and subsequently updated through repeated interactions with the environment through optimisation of evidence (minimisation of free energy) and maximisation of external and internal stimuli (Friston, 2012).

1.3 Learning function of decision making under uncertainty

When we are faced for the first time with making a decision, in a previously unknown context, decision making occurs under a context of high uncertainty (ambiguity). In this situation we do not know the probability distribution of the options that allow us to reach the best expected outcome. Friedman's neoclassical economics suggests that when an individual makes a decision, first, he or she constructs a list of all the possible options he or she can choose from and ranks them from the best to the worst. Second, the individual makes a selection from the highest ranked options (Glimcher & Fehr, 2013).

On the other hand, neuroeconomists have defined the process of making a decision as a two-

stage mechanism: First, the assignment of a subjective value to the options to be chosen (option value). Second, the results of the choice are evaluated (reward value). Considering that the human being is risk averse and always wishes to reduce uncertainty, an individual creates an internal model of the system where he predicts what would be the probability distribution to make his first decision (Kable & Glimcher, 2009), however, it is likely that the internal model that the individual has initially designed is different from the actual model of the system, and therefore, it is necessary to explore the task to compare the result obtained from his choice with the expected outcome. The reward Prediction Error (PE) consists of the difference between the reward received and the expected reward, mathematically expressed as:

$$PE = (\textit{Obtein Result} - \textit{Expected Result})$$

This factor allows us to update the value of the option because if our prediction is wrong the result obtained will be far from the expected result, which will indicate that the option we chose does not allow us to reach the best expected result, and therefore, the value of the chosen option is modified, that is, there is a learning function of the value of the option modulated by the magnitude of the prediction error, for which the presence of feedback in the task is necessary. On the contrary, if our prediction is assertive and the option, we choose delivers the expected outcome there will be no update of the option value and therefore no increase in the learning function (Schultz, 2016) (see Figure 1.2).

Scientific evidence shows that when we explore the decision-making task we learn the probability distribution of the options, which means that there is an integration of the prediction error that allows us to update the option value caused by an increase in the learning function, and therefore, our choices are better or more accurate in obtaining the expected outcome (Diederen, Spencer, Vestergaard, Fletcher, & Schultz, 2016).

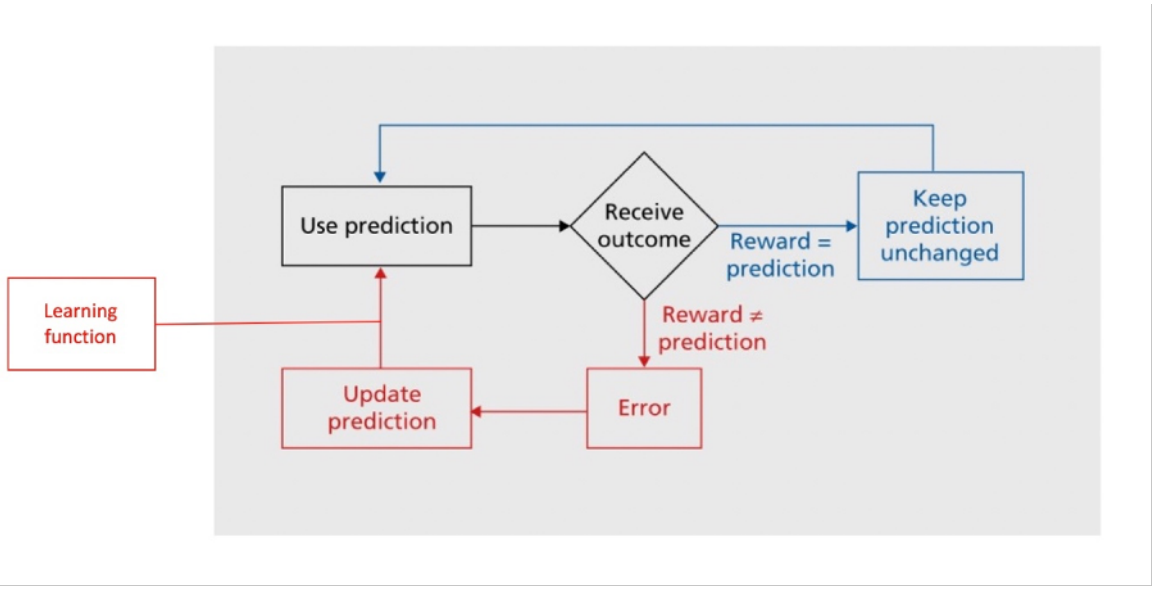

Figure 1.2: **Modification of learning scheme by prediction error.** Red: there is a prediction error when the reward differs from its prediction. Blue: no error exists when the outcome matches the prediction and the behavior remains unchanged (Schultz, 2016).

1.4 Model of decision making

Neuroscience has focused on the study of internal order choices that focuses on understanding the cognitive, behavioral and psychological processing that underlies individual decision making. To elucidate how humans establish preferences in our choices. In 1654 Pasca and Fermat constructed the first behavioral formulations of decision making by establishing expected value *(EV)* as the product of gain *(x)* and probability of occurrence *(p)*. This model estimates that individuals seek to maximize the expected value utilities, therefore it assumes that subjects prefer options with high probability of occurrence and low outcome to options with low probability of occurrence and high reward/payment. Later, the Prospective theory of Kahneman and Tversky (1979 and 1992) proposes a model of decision making under uncertainty that establishes three basic principles:

1. The evaluation of an outcome is relative to the individual's usual wealth, which is called "status quo".

2. Sensitivity to change is decreasing according to subjective valuation.

3. There is loss aversion, that is, the weighting of losses outweighs the weighting of gains, as

Adam Smith (1759; 1982: 213) pointed out, the effect of a loss is greater than that of a gain.

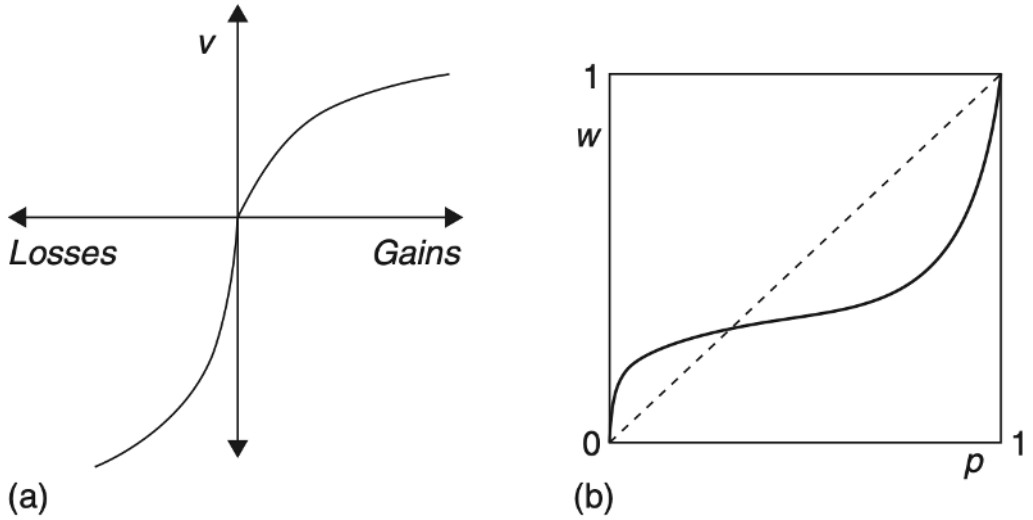

Figure 1.3: **Representative value and weighting functions from prospect theory.** ***(a)*** A hypothetical prospect theory value function illustrating concavity for gains, convexity for losses, and a steeper loss than gain limb. ***(b)*** A hypothetical prospect theory weighting function illustrating its characteristics inverse-S shape, the tendency to overweight low probabilities and underweight moderate to large probabilities, and the tendency for weights of complementary probabilities to sum to less than 1. (Extracted image from (Glimcher & Fehr, 2013))

1.5 Neurobiological activity associated with decision-making in contexts of stable uncertainty and volatility

Neuroscientists have endeavoured to elucidate the cognitive mechanisms that allow us to construct the value of the option we will choose when making a decision. From von Neurmann's expected utility theory to reinforcement-based learning theories, it has been concluded that an individual is able to make a decision by integrating several dimensions or qualities of an option into a single measure of subjective value and, as mentioned above, the value of choices can only be constructed after we have had the opportunity to explore the task and subsequently receive feedback on our decisions. This allows us to compare the expected value of the choice and the

obtained value (Kable & Glimcher, 2009), i.e. the prediction error (PE) updates the value of the choice via the learning function. The mathematical expression that could demonstrate the scaling of the learning function in a decision making context under stable uncertainty could be expressed as follows:

$$f(PE) = \frac{PE}{Uncertainty}$$

Decision-making experiments have revealed that the basic mechanisms underlying the option value construction process involve ventromedial and striate prefrontal brain areas. During the option choice period, neural activity has been observed in lateral prefrontal areas and in the parietal cortex cohen2002reward,kable2009neurobiology. It has also been studied how the cingulate cortex specifically participates in the encoding of the relative value of an option, which corresponds to the present value of a short-term option, which is constructed from the current choice and the next choice. The areas associated with this function are the ventromedial prefrontal cortex (vmPFC), the medial cingulate cortex (mACC) and the posterior cingulate cortex (pACC). The encoding of the option with the highest long-term value would occur in the dorsal anterior cingulate cortex (adACC) (Boorman, Rushworth, & Behrens, 2013).

Studies of decision making in contexts of stable uncertainty have evidenced that there are changes in BOLD signaling in dopaminergic neurons in this process (D'Ardenne, McClure, Nystrom, & Cohen, 2008; Knutson & Wimmer, 2007) and it has been estimated that Dopamine interacts with other neuromodulators to influence choices (Doya, 2008). It has been observed that the prediction error encoding process is modulated by dopaminergic circuits (Montague, Dayan, & Sejnowski, 1996; Schultz, Apicella, & Ljungberg, 1993) and that in probabilistic decision-making tasks there is a greater activation of the Substance Nigra/VTA complex when the prediction error is more informative. Additionally, it has been shown that when encoding prediction error there is a simultaneous activation in VTA/Sustancia Nigra and Ventral Striatum in the Prefrontal cortex, assuming a connectivity between both areas (Diederen et al., 2016).

The volatility context implies a change in the a priori known world, therefore, when contingencies change the error in prediction increases, and therefore, and it is necessary for the decision maker to be able to observe that this is due to a change in one of the factors of the probability distribution of the options, either the mean, the standard deviation or both. The learning function in the context of volatility can be described as:

$$f(PE) = \frac{PE}{Uncertainty} * \Delta Uncertainty$$

Studies in volatility (or reverse learning) contexts have revealed an activation of the Locus Coereleus (LC) nucleus showing that phasic activity releases the neuromodulator Noradrenaline and is estimated to encode the outcome of our decisions, while in its tonic activity it would preferentially encode behavioral change (Aston-Jones & Cohen, 2005; Angela & Dayan, 2005; Dayan & Yu, 2006; Sales, Friston, Jones, Pickering, & Moran, 2019) possibly causing a further increase in learning function in volatile contexts, i.e., increased learning when change in the conception of the familiar world occurs (Dayan & Jyu, 2003). The neurobiological mechanism by which the LC nucleus would participate in encoding prediction error variance is unknown but a Resting-state study demonstrates that there is connectivity between LC and the fronto-parietal network that is usually activated in choice encoding tasks in uncertain contexts, the role of which is still unclear (Zhang, Hu, Chao, & Li, 2016).

1.5.1 Neural activity associated to Prediction Error

Studies using event-related brain potentials (ERPs) have revealed that the human brain is capable of evaluating the outcome of actions within a few 100 ms. Error-related negativity (ERN; (Falkenstein, 1990; Gehring, Coles, Meyer, & Donchin, 1990)) and feedback-related negativity (FRN; (Miltner, Braun, & Coles, 1997)) have been observed to be elicited by erroneous responses and by negative feedback or losses, respectively. Another component of the ERP that has been

shown to carry information important for reward processing is the feedback-related P300, a parietally distributed positivity (Yeung & Sanfey, 2004; Polezzi, Sartori, Rumiati, Vidotto, & Daum, 2010).

Yeung and Sanfey (2004) studied the effects of winning or losing large or small amounts of money on FRN and P300 and concluded that only P300 was affected by the amount of monetary loss, whereas FRN was insensitive to the magnitude of the outcome.

Both ERN and FRN have been shown to reflect a degree of theta phase consistency and increased power in the medial frontal cortex (Bernat, Nelson, Holroyd, Gehring, & Patrick, 2008; Cavanagh, Cohen, & Allen, 2009; Cohen & Ranganath, 2007; Marco-Pallares et al., 2008; Trujillo & Allen, 2007), supporting the main postulate of Holroyd and Coles' (2002) reinforcement learning theory that these two ERPs reflect high-level error processing. Theta oscillations may represent a general operating mechanism of the medial and lateral frontal cortexes involved in action monitoring and behavioral adjustment.

The study by Billeke et al., (Billeke et al., 2020) shows activity in the amplitude of beta oscillations in the anterior insular cortex that is modulated by the probability of the valence of performance feedback (positive or negative) given the context. In addition, feedback valence was encoded by the delta waves that modulate the power of beta oscillations. Connectivity and causal analysis showed that beta oscillations transmit feedback information signals to the medial frontal cortex. These results reveal that structured oscillatory activity in the anterior insula encodes feedback information about performance.

Another recent study shows that reward and punishment prediction errors (PEs) correlate positively with broadband gamma activity (BGA) with outcome (reward or punishment vs. nothing) and negatively with expectation (reward or punishment prediction). Reward EPs were better signaled in some regions (such as ventromedial prefrontal cortex and lateral orbitofrontal cortex), and punishment EPs in other regions (such as anterior insula and dorsolateral prefrontal cortex) (Gueguen et al., 2021).

References

Angela, J. Y., & Dayan, P. (2005). Uncertainty, neuromodulation, and attention. *Neuron*, *46*(4), 681–692.

Aston-Jones, G., & Cohen, J. D. (2005). Adaptive gain and the role of the locus coeruleus–norepinephrine system in optimal performance. *Journal of Comparative Neurology*, *493*(1), 99–110.

Bernat, E. M., Nelson, L. D., Holroyd, C. B., Gehring, W. J., & Patrick, C. J. (2008). Separating cognitive processes with principal components analysis of eeg time-frequency distributions. In *Advanced signal processing algorithms, architectures, and implementations xviii* (Vol. 7074, pp. 240–249).

Billeke, P., Ossandon, T., Perrone-Bertolotti, M., Kahane, P., Bastin, J., Jerbi, K., … Fuentealba, P. (2020). Human anterior insula encodes performance feedback and relays prediction error to the medial prefrontal cortex. *Cerebral Cortex*, *30*(7), 4011–4025.

Bland, A. R., et al. (2012). Different varieties of uncertainty in human decision-making. *Frontiers in neuroscience*, *6*, 85.

Boorman, E. D., Rushworth, M. F., & Behrens, T. E. (2013). Ventromedial prefrontal and anterior cingulate cortex adopt choice and default reference frames during sequential multi-alternative choice. *Journal of Neuroscience*, *33*(6), 2242–2253.

Cavanagh, J. F., Cohen, M. X., & Allen, J. J. (2009). Prelude to and resolution of an error: Eeg phase synchrony reveals cognitive control dynamics during action monitoring. *Journal of Neuroscience*, *29*(1), 98–105.

Clark, A. (2013). Whatever next? predictive brains, situated agents, and the future of cognitive science. *Behavioral and brain sciences*, *36*(3), 181–204.

Cohen, M. X., & Ranganath, C. (2007). Reinforcement learning signals predict future decisions. *Journal of Neuroscience*, *27*(2), 371–378.

D'Ardenne, K., McClure, S. M., Nystrom, L. E., & Cohen, J. D. (2008). Bold responses reflecting dopaminergic signals in the human ventral tegmental area. *Science*, *319*(5867), 1264–1267.

Dayan, P., & Jyu, A. (2003). Uncertainty and learning. *IETE Journal of Research*, *49*(2-3), 171–181.

Dayan, P., & Yu, A. J. (2006). Phasic norepinephrine: a neural interrupt signal for unexpected events. *Network: Computation in Neural Systems*, *17*(4), 335–350.

Diederen, K. M., Spencer, T., Vestergaard, M. D., Fletcher, P. C., & Schultz, W. (2016). Adaptive prediction error coding in the human midbrain and striatum facilitates behavioral adaptation and learning efficiency. *Neuron*, *90*(5), 1127–1138.

Domenech, P., Redouté, J., Koechlin, E., & Dreher, J.-C. (2018). The neuro-computational architecture of value-based selection in the human brain. *Cerebral Cortex*, *28*(2), 585–601.

Doya, K. (2008). Modulators of decision making. *Nature neuroscience*, *11*(4), 410–416.

Falkenstein, M. (1990). Effects of errors in choice reaction tasks on the erp under focused and divided attention. *Psychophysiological brain research*.

Friston, K. (2012). The history of the future of the bayesian brain. *NeuroImage*, *62*(2), 1230–1233.

Gehring, W. J., Coles, M. G., Meyer, D. E., & Donchin, E. (1990). The error-related negativity: an event-related brain potential accompanying errors. *Psychophysiology*, *27*(4), S34.

Glimcher, P. W., & Fehr, E. (2013). *Neuroeconomics: Decision making and the brain*. Academic Press.

Gueguen, M., Lopez-Persem, A., Billeke, P., Lachaux, J.-P., Rheims, S., Kahane, P., … Bastin, J. (2021). Anatomical dissociation of intracerebral signals for reward and punishment prediction errors in humans. *Nature communications*, *12*(1), 1–12.

Huettel, S. A., Song, A. W., & McCarthy, G. (2005). Decisions under uncertainty: probabilistic context influences activation of prefrontal and parietal cortices. *Journal of Neuroscience*, *25*(13), 3304–3311.

Kable, J. W., & Glimcher, P. W. (2009). The neurobiology of decision: consensus and controversy. *Neuron*, *63*(6), 733–745.

Kahneman, D., & Tversky, A. (2013). Prospect theory: An analysis of decision under risk. In *Handbook of the fundamentals of financial decision making: Part i* (pp. 99–127). World Scientific.

Knill, D. C., & Pouget, A. (2004). The bayesian brain: the role of uncertainty in neural coding and computation. *TRENDS in Neurosciences*, *27*(12), 712–719.

Knutson, B., & Wimmer, G. E. (2007). Splitting the difference: how does the brain code reward episodes? *Annals of the New York Academy of Sciences*, *1104*(1), 54–69.

Ma, W. J., & Jazayeri, M. (2014). Neural coding of uncertainty and probability. *Annual review of neuroscience*, *37*, 205–220.

Marco-Pallares, J., Cucurell, D., Cunillera, T., García, R., Andrés-Pueyo, A., Münte, T. F., & Rodríguez-Fornells, A. (2008). Human oscillatory activity associated to reward processing in a gambling task. *Neuropsychologia*, *46*(1), 241–248.

Miltner, W. H., Braun, C. H., & Coles, M. G. (1997). Event-related brain potentials following incorrect feedback in a time-estimation task: evidence for a "generic" neural system for error detection. *Journal of cognitive neuroscience*, *9*(6), 788–798.

Montague, P. R., Dayan, P., & Sejnowski, T. J. (1996). A framework for mesencephalic dopamine systems based on predictive hebbian learning. *Journal of neuroscience*, *16*(5), 1936–1947.

Polanía, R., Krajbich, I., Grueschow, M., & Ruff, C. C. (2014). Neural oscillations and synchronization differentially support evidence accumulation in perceptual and value-based decision making. *Neuron*, *82*(3), 709–720.

Polezzi, D., Sartori, G., Rumiati, R., Vidotto, G., & Daum, I. (2010). Brain correlates of risky decision-making. *Neuroimage*, *49*(2), 1886–1894.

Quirk, G. J., & Mueller, D. (2008). Neural mechanisms of extinction learning and retrieval. *Neuropsychopharmacology*, *33*(1), 56–72.

Rangel, A., Camerer, C., & Montague, P. R. (2008). A framework for studying the neurobiology of value-based decision making. *Nature reviews neuroscience*, *9*(7), 545–556.

Sales, A. C., Friston, K. J., Jones, M. W., Pickering, A. E., & Moran, R. J. (2019). Locus coeruleus tracking of prediction errors optimises cognitive flexibility: An active inference model. *PLoS computational biology*, *15*(1), e1006267.

Schultz, W. (2016). Dopamine reward prediction-error signalling: a two-component response.

Nature reviews neuroscience, *17*(3), 183–195.

Schultz, W., Apicella, P., & Ljungberg, T. (1993). Responses of monkey dopamine neurons to reward and conditioned stimuli during successive steps of learning a delayed response task. *Journal of neuroscience*, *13*(3), 900–913.

Sutton, R. S., & Barto, A. G. (2018). *Reinforcement learning: An introduction*. MIT press.

Trujillo, L. T., & Allen, J. J. (2007). Theta eeg dynamics of the error-related negativity. *Clinical Neurophysiology*, *118*(3), 645–668.

Yeung, N., & Sanfey, A. G. (2004). Independent coding of reward magnitude and valence in the human brain. *Journal of Neuroscience*, *24*(28), 6258–6264.

Zhang, S., Hu, S., Chao, H. H., & Li, C.-S. R. (2016). Resting-state functional connectivity of the locus coeruleus in humans: in comparison with the ventral tegmental area/substantia nigra pars compacta and the effects of age. *Cerebral Cortex*, *26*(8), 3413–3427.

Hypothesis

Hypothesis 1

The parietal cortex causally contributes to valuing ambiguous information during decision-making.

Hypothesis 2

The parietal cortex participate in the modulation of the learning rate in volatile context.

Chapter 2

A causal role for the parietal cortex in ambiguity computations in humans

Gabriela Valdebenito-Oyarzo[1], María Paz Martinez-Molina[1], Patricia Soto-Icaza[1], Alejandra Figueroa-Vargas[1], Josefina Larraín-Valenzuela[1], Francisco Zamorano[1,2], Ximena Stecher[2], Antonie-Valero-Cabre[3,4,5], Rafael Polania[6] and Pablo Billeke[1 1]

[1]Laboratory of Social Neuroscience and Neuromodulation, Centre for Research in Social Complexity, (neuroCICS), Faculty of Government, Universidad del Desarrollo, Santiago, Chile.

[2]Department of Imaging, Clinica Alemana De Santiago, Chile.

[3]Causal Dynamics, Plasticity and Rehabilitation Group, FRONTLAB team, Institut du Cerveau et de la Moelle Epinière (ICM), CNRS UMR 7225, INSERM U 1127 and Sorbonne Université, Paris, France.

[4]Laboratory for Cerebral Dynamics Plasticity and Rehabilitation, Boston University, School of Medicine, Boston, MA, USA.

[5]Cognitive Neuroscience and Information Technology Research Program, Open University of Catalonia (UOC), Barcelona, Spain.

[6] Decision Neuroscience Lab, Department of Health Sciences and Technology, ETH Zurich, Zurich,

[1]CONTACT Pablo Billeke Email: pbilleke@udd.cl

Switzerland.

Highlights

(i) Humans assign unknown probabilities to outcomes during decision-making under ambiguity.

(ii) Parietal cortex activity correlates with ambiguity computations during decision-making.

(iii) Lateral frontal activity in the inferior frontal junction (IFJ) correlates with prediction errors emerging from ambiguity computations.

(iv) Perturbation of parietal activity increases the assignment of ambiguity levels to unknown probabilities and reduces frontolateral theta oscillations in the IFJ associated with prediction error.

Abstract

Humans must often estimate reward values in the presence of ambiguous information and determine the best course of action on such a basis. The degree of uncertain information is related to levels of activity in the parietal cortex, however, its specific computations and causal role remain unknown. We tested the hypothesis that the parietal cortex is causally related in the computation of ambiguous probabilities during decision-making, studied via fMRI and concurrent TMS-EEG recordings. We found that activity in the parietal cortex correlated with the degree of ambiguity assigned to subjective probability estimates. Moreover, disruption of parietal activity selectively increased the assignment of unknown probabilities to outcomes during ambiguity decisions and modulated frontal theta oscillations related to prediction error signals emerging from ambiguous choices. These results contribute to evidence supporting a fundamental causal role for the parietal cortex in the computations of ambiguous information during risky decisions and learning in humans.

Keywords: Decision-Making; Prediction Error; Ambiguity; Parietal Cortex.

2.1 Introduction

How do we decide when faced with options where we do not know the outcome? For example, if we visit a city for the first time, how do we decide which restaurant prepares the pizza the way we like it? Making choices on the basis of incomplete information about the potential outcomes is something that human beings have to deal with almost every day. Despite the common occurrence of this scenario in ecological settings, organisms generally try to avoid such situations, a phenomenon known as ambiguity aversion (?, ?, ?, ?, ?). In this regard, ambiguity refers to a type of uncertainty, which involves situations where a degree of ignorance about the probability of the results of each option exists (?, ?). Therefore, depending on the individual's knowledge about the environment, the predictability of the consequences of each option changes, which in turn varies the degree of uncertainty. How humans incorporate this type of incomplete information when making decisions, and its underlying neurobiological mechanisms remain unclear.

Faced with decision-making, individuals weigh or value each option based on available information, such as the knowledge about the probability of the consequence of each option and its associated reward. Among other brain areas, this value processing relies on a well-known brain network, which involves the ventromedial prefrontal/ orbitofrontal cortex and the ventral striatum (?, ?, ?, ?). In addition, other sets of brain areas, including the intraparietal sulcus (IPS) and the dorsal posterior parietal cortex (PPC) (?, ?; Huettel et al., 2005; ?, ?), have been identified when comparing different degrees of uncertainty during decision making. Specifically, activity in the lateral frontal and parietal areas correlates with both the degree of uncertainty (Huettel et al., 2005) and the update-value process that reduces the uncertainty (?, ?). Moreover, recent studies in non-human animals have demonstrated a critical role of the parietal cortex in the encoding of the possible reduction of uncertainty that an action is expected to yield during perceptual decision-making (?, ?). In contrast, findings in humans indicate that parietal activity could be related to surprise signaling without a clear influence in both value processing and updating (?, ?). Hence, no specific causal role of parietal regions during value-based decision-making under ambiguity has been determined to date.

Once individuals make a decision, they evaluate whether their choice meets their predictions, generating a prediction error signal that serves to update value and learn (Gueguen et al., 2021; Kable & Glimcher, 2009; ?, ?; Rangel et al., 2008). After a decision, it has been demonstrated that the parietal region sustained

effective connectivity with the lateral prefrontal cortex, biasing future decisions (?, ?). Unexpected outcomes in an uncertain environment have been associated with both lateral prefrontal activity using fMRI (?, ?) and theta activity using EEG recordings (?, ?, ?). Indeed, several works exploring oscillatory activity have demonstrated that frontal theta activity correlates with prediction error and guides future decisions in uncertain situations (?, ?, ?, ?, ?). Although connectivity between parietal and frontal regions seems critical for decision making and accurate value representation (?, ?, ?), the influence of parietal activity in frontal prediction-error signals is not yet known.

Considering the current evidence, we hypothesize here that the parietal cortex causally contributes to valuing ambiguous information during decision-making. To test this, we used a probabilistic decision-making task with ambiguity and elaborated an experimental approach that sequentially built and integrated knowledge that came from an fMRI experiment and a subsequent TMS-EEG experiment. First, we fitted computational cognitive models of behavioral outcomes to infer underlying computations. Second, we mapped the models' components in the cortex using model-based fMRI. We next assessed the causal involvement of these identified cortical areas using TMS stimulation. Finally, we identified the oscillatory mechanisms underlying TMS disruption using model-based EEG analyses. Using such an approach, we found that participants assigned some proportion of the unknown probabilities to objective, known probabilities during decision-making under ambiguity. This process correlated with parietal activity in both the IPS and the PPC. The prediction error signal related to the ambiguity assignment scaled with the activity of the lateral frontal area (inferior frontal junction, IFJ). Moreover, the perturbation via TMS of both the IPS and the PPC increased the assignment processing, in such a way that the individual behaved as if the decisions were less ambiguous. Additionally, the IPS perturbation reduced the lateral frontal theta activity in the IFJ involved in the prediction error related to ambiguous probabilities. These results indicate a causal role of the parietal cortex in the computation of ambiguous information during decision-making under uncertainty.

2.2 Results

2.2.1 Behavioral Model

In our behavioral task, participants had to choose between two options. Each option had different and complementary probabilities of being rewarded, and they were associated with varying magnitudes of reward (Figure 1). In half of the trials, actual probabilities were partially hidden (from 40% to 80% of occlusion, generating different degrees of ambiguity P_a=0, 0.4, 0.5, 0.6, 0.7, 0.8). We expected that, during the ambiguity condition, participants would assign some proportion of the hidden area Pa to the visible probability (we called that objective probability P_{obj}). This assignment can be described with two parameters, namely τ_i and τ_b, which range between 0 to 1. τ_i represents the proportion of the hidden area P_a that is effectively assigned to the P_{obj}, and bthe bias by which this assignment is assigned to one option or another (see Figure 1B). The final probability that the participants take into account when they make a decision is P_{all}, which is given by the following equations.

$$P_{all} = P_{obj} + P_{ass}$$

$$P_{att_l} = P_a * \tau_b * \tau_i$$

$$P_{att_r} = P_a * (1 - \tau_b) * \tau_i$$

τ_i close to zero indicates a process in which participants do not assign the unknown probabilities to the objective (known) probabilities, incorporating the hidden area as an additional factor in the decision-making process. In other words, the uncertainty introduced by the hidden area is taken into account in the decision process as an unknown probability. In the opposite case, when τ_i is near to one, the uncertainty given by the hidden area is mainly ignored in the decision-making process, being assigned to the objective probabilities. In other words, participants behave as if there is no ambiguity in the probabilities.

To test whether individuals make such computations, we fitted several cognitive computational models using prospect theory (as in prior work (?, ?)) since they have demonstrated better behavior and neural

adjustment than other value models (?, ?). For the adjustment, we used a hierarchical Bayesian approach (?, ?, ?). The best-fitted model (e.i., the smallest Deviance Information Criterion, DIC, see Figure 2) presents a fixed τ_b = 0.5 and τ_i as a free parameter (M(τ_b=0.5, τ_i, β_0=0), mean τ_i, $\hat{\tau}_i$ = 0.77 [0.67 - 0.91], p_{MCMC}< 0.003 testing τ_i>0.5; p_{MCMC} is a p-value derived by comparing the posterior distributions of the estimated parameters sampled via Markov Chain Monte Carlo, interval indicating the 95% high-density intervals, HDI). This means that individuals assigned a large proportion of unknown probabilities to objective probabilities without biasing either option.

In order to provide more evidence for non-biased assessment, we evaluated models that included parameters that captured such bias. In the best-fitted model that included τ_b as a free parameter, it was not different from 0.5 (M(τ_b, τ_i, β_0), $\hat{\tau}_b$=0.47 [0.42 - 0.52], p_{MCMC}=0.25). We also tested another bias parameter, $\tau_{b'}$, that represents an assignment biased to the greatest R_w rather than laterality (left option, how it is represented by τ_b). Similarly, in the best-fitted model that includes $\tau_{b'}$ as a free parameter, it was not different from 0.5 (M($\tau_{b'}$, τ_i, β_0), $\hat{\tau}_{b'}$=0.51 [0.47 -0.56], p_{MCMC}=0.46). Therefore, participants assign probability from the ambiguity area to the objective probability without a particular bias related to the laterality or reward of each option.

Using the parameter readout from the best-fitted model, we carried out several simulations with different τ_i each, in the same decisions that the experimental participants were exposed to, and selected those simulations with the greater total outcome obtained (5% highest performance simulations out of 150000). The simulations that obtained more reward had a τ_i closer to 1 (mode = 0.97, median = 0.92, 95% HDI = [0.5 - 0.999]). This means that large assignments optimize the payoff in this particular setting.

To obtain further evidence for this computation and rule out any possible skewness given by adjustment methodology we probe other models assuming a τ_i=1 and τ_b=0.5 (P_{alll}=P_{obj_l} + P_a/2, see details in the Materials and Method section, and using likelihood-based model selection. Thus, we fitted several mixed logistic models with different parameters and selected the model with the best data adjustment (i.e., the smallest Akaike information criterion, AIC, see supplementary Table 1). The fitted model is presented as a "Logistic Model" in Figure 2A and Supplementary Table 2. These results indicate that the participants carried out a high assignment of P_a (e.i., τ_i 1) since the interaction P_{all_l}:P_a was not significant (-2.3, SEM=2.4, z=-1.3, df=1493, p=0.1). However, its negative coefficient could indicate some distance from this to one. That is, participants took into account to some extent the uncertainty of ambiguous information.

Additionally, since P_a was also not significant (1.3, SEM: 1.2, z=1.0, df=1493, p=0.2), it is possible to expect a $\tau_b \sim 0.5$. Finally, this model does not present the interaction $Rw_l : P_a$, but in the best-fitted model that includes this interaction, it proved not significant, indicating that the ambiguity did not have a major impact on the reward estimation (z=-1.4, df=1493, p=0.13, see supplementary Table 1). Note that these models fit worse than the cognitive computational models (using DIC for comparison, see Figure 2A). Overall, these analyses indicate that individual effectivity assigned a large proportion of ambiguous information to known probabilities in order to make a decision and that the computational cognitive model better captures the behavioral variability.

fMRI

2.2.2 Value-related activity during decision making

In order to identify brain regions underpinning the assignment of probability in conditions of ambiguity, we first modeled the BOLD signal during the decision phase using Rw, P_{obj} , and P_{as} of the selected option as independent regressors together with control regressors in order to avoid activity contributed by the differences in difficulty between conditions (namely, reaction time, ambiguity as a categorical regressor, see Methods for more details). For these analyses we first probed several ways to calculate Pas as a regressor, selecting the one that was orthogonalized to P_{obj} regressor and normalized to reduce the collinearity with P_a (see Methods). The comparison between these ways to calculate the P_{as} as a regressor is shown in Supplementary Figure 1. Additionally, we estimated the BOLD activity that correlates with the degree of ambiguity, by means of an independent model for the regressor P_a (due to the interdependence among P_{obj}, P_{as}, and P_a, see Methods). Reward magnitude of the chosen option generates greater activity in several brain regions, including the ventral striatum (Figure 3 and Supplementary Table 2). The P_obj and P_{as} regressors showed a correlation in the IPS and in the posterior part of the frontal gyrus compatible with the frontal eye field (FEF). The P_{obj} regressor revealed activity in the left IPS, while the Pas regressor yielded activity in both right frontal regions and bilateral parietal regions. All these regions showed a modulation related to the degree of ambiguity P_a (see the insert in Figure 3A).

2.2.3 Feedback-related activity

Using the same approach, we investigated brain activity related to feedback processing. In this model, we used several regressors (see Materials and Methods), separating the activity tied to the probability prediction error given by P_{as} (using unsigned prediction error, $uPE\text{-}P_{as}$) from the activity of the probability prediction error given by P_{obj} (using unsigned prediction error, $uPE\text{-}P_{obj}$). We found a bilateral activity correlated with $uPE\text{-}P_{as}$ in the posterior portion of the inferior frontal gyrus/sulcus compatible with the inferior frontal junction (IFJ). The fact of winning generated activity in several brain regions, including the IFJ and the ventral striatum. Additionally, the magnitude of the obtained reward correlated with the activity in the ventromedial prefrontal cortex. No activity correlated with uPE-Pobj reached statistical significance.

TMS-EEG

2.2.4 Parietal inhibition increased the assignment of ambiguous probability

In order to test the causal role of the parietal cortex in the brain network that assigns probability from unknown probabilities during decision making, we carried out a subsequent interleaved TMS-EEG session while participants carried out the same task used for the fMRI experiments. We targeted two regions in the parietal cortex that displayed significant activity during the decision period in the fMRI experiments (Figure 4 A). The first one corresponds to the dorsal posterior parietal cortex (PPC, MNI: [14 -64 56]) that showed activity related to P_a, but neither to P_{as} nor to P_{obj}. The second region was to the right intraparietal sulcus (IPS, MNI:[36, -46, 56]) that correlated with both P_{as} and P_a, but not to P_{obj} (see Figure 2 and 4). Active stimulation in the vertex of the scalp was used as a control condition. Since prior work indicates that the parietal region sustains effective connectivity with the lateral prefrontal cortex after the decision and that this activity biases future decisions (?, ?), an online TMS design based on a doublet of pulses (separated by 100 ms, hence covering a time window of 100-200 ms) was delivered trial-by-trial after the decision-making process (200 ms prior to the feedback onset). The rationale behind those choices was to disrupt the signal required to encode the prediction error during feedback and, by virtue of

such effect, interfere in the decision-making process of future trials.

As mentioned above, since TMS stimulation occurred after decision making, the main aim of this experiment was to look for decreases in the frontal theta activity related to prediction error (see below). Secondarily, we aimed to investigate the potential intra-session cumulative impact of trial by trial TMS on behavioral effects. Accordingly, we fitted the selected cognitive model from the fMRI experiments (Logistic and M(τ_b=0.5, τ_i, β_0=0), Figure 2) in the 20 final trials of each 40-trials run of the same TMS stimulation (see Methods). Comparing the model fitted for each TMS stimulation, we found that both the IPS TMS stimulation and the PPC TMS stimulation generated an significant increase in $\hat{\tau}_i$ in comparison with vertex stimulation (Figure 4B, Vertex $\hat{\tau}_i$=0.59 [0.49 0.67]; IPS $\hat{\tau}_i$=0.81 [0.67 0.92]; PPC $\hat{\tau}_i$=0.88 [0.73 0.99], differences Vertex-PPC p_{MCMC}< 0.001, Vertex-IPS p_{MCMC}< 0.001, IPS-PPC p_{MCMC}> 0.3 , Bonferroni corrected). Notably, none of the other parameters of the model were modulated by TMS stimulation (see supplementary Table 4). In order to evaluate a potential attention bias generated by the parietal inhibition (?, ?), we also fitted models with additional parameters that captured possible lateral bias (namely: β_0 and τ_b). All the models that include those parameters fitted worse than the selected one, and these parameters did not show to be different to zero or 0.5 respectively (see supplementary Table 5). These results indicate that the interruption of parietal activity specifically affects the assignment of ambiguous probabilities and not other computations during decision-making processing.

In a similar way as in the fMRI experiment, to rule out any possible skewness given by adjustment methodology, we also fitted the selected logistic model. This model showed an effect for TMS stimulation (collapsed IPS and PPC stimulation) specifically for ambiguity interaction (P_a*TMS, 3.1, SEM:1.3, Z-value 2.3, p=0.01; P_a*P_{all}*TMS, -5.4, SEM:2.6, Z-value -2.0, p=0.03; see Supplementary Table 6). The model individualized for each parietal targeted region showed the same direction of the effect but did not show significance (Supplementary Table 6). Note that for all of these models, the TMS regressors did not show a statistically significant effect, indicating no evidence for laterality bias (p>0.14, Supplementary Table 3, see (?, ?)). These results give robustness to the casual participation of the parietal cortex in ambiguity computation without effect laterality bias.

2.2.5 Parietal inhibition interrupts the prediction error signal related to assigned probability

Using a similar model as in the fMRI experiments, we investigated brain oscillatory activity related to feedback processing. In this model, we used several regressors (see Materials and Methods) separating the activity of the probability prediction error given by P_{as} (using unsigned prediction error, uPE-P_{as}) from the activity of the probability prediction error given by P_{obj} (using unsigned prediction error, uPE-P_{obj}). Also, the model included dummy regressors for the IPS-TMS stimulation and the PPC-TMS stimulation conditions and the interaction between each TMS stimulation condition and the task-related regressors. We explored frontal electrodes where theta activity related to prediction error has been described in prior work (?, ?, ?, ?, ?). For both uPE regressors, we found a significant modulation (Figure 5). During vertex stimulation, we found an oscillatory activity in the alpha/beta range that was associated to uPE-P_{obj} (8-16 Hz, 0.2 - 0.3 s post feedback, cluster-based permutation test in frontal electrodes, CTD p=0.05, p<0.001), whereas a theta activity was associated to uPE-P_{as} (3-6 Hz, 0.4 - 0.5 s post feedback, cluster-based permutation test in both frontal electrodes and in whole scalp analysis, CTD p=0.05, p<0.001). With regards to the interaction between these regressors and TMS stimulation regressors, we found that only the IPS stimulation generated a modulation in the theta activity related to uPE-P_{as}. Source analysis revealed that the modulation reported for the IPS-TMS stimulation condition involved a similar area to that found in the fMRI experiments in the IFJ (see the inserts in Figure 5C). Overall, the EEG results indicated that the disruption of IPS activity before feedback affects the theta activity in IFJ evoked by the prediction error built with the assigned ambiguous probability. Therefore, the parietal cortex causally participates in ambiguity computation, and parietal to frontal interaction seems necessary to signal outcome prediction given by this ambiguity computation.

2.3 Discussion

The results of this study provide evidence for a causal role of the parietal cortex during decision-making under ambiguous conditions. Using consecutive analyses and sequentially informed fMRI and EEG-TMS experiments, we explored the cognitive computations that underlay decision-making in ambiguous situ-

ations and tested the casual involvement of the parietal cortex in such a computation. In particular, we found that the parietal cortex activity correlates with the degree of ambiguity of the decision, reflecting the encoding of the value of the ambiguous probabilities. In this valuation, participants assign a proportion of unknown probabilities to the objective, observable probabilities. In other words, this value is the additional subjective predictability of the outcome assigned from the unknown information. Indeed, cognitive modeling performed in the current study strongly suggests that this process is part of the computation participants made when faced with ambiguous decisions, specifically affected by the interference of the parietal cortex evoked by time-locked TMS perturbation. The valuing of ambiguous information influences the prediction of subsequent outcomes. In the fMRI experiment, the activity in the IFJ correlated with the prediction error generated by the assigned ambiguity probability during outcome evaluation. Indeed, in the EEG-TMS experiments, the parietal perturbation caused a decrease of lateral frontal theta activity, in turn, evoked by the prediction error of ambiguous information in quite similar areas of that identified in the fMRI experiment.

In accordance with current research, our results indicate that parietal activity senses outcome likelihood and predictability. Beyond the known role of the parietal region in perceptual decision-making (?, ?), increasing evidence has related parietal activity to value during decision making under conditions of uncertainty (?, ?, ?). Non-human primate studies have shown that parietal regions, such as the intraparietal sulcus (IPS), link the probability to obtain a reward with a specific action (e.g., the direction of the saccade (?, ?)). Neurons of the dorsal parietal region have also shown activity for a combination of reward magnitude and probability (?, ?). Moreover, some parietal neurons are specifically modulated by the expected utility of the options (?, ?). In this context, our results show differential modulations of the parietal cortex associated with the chosen option probability provided by the objective and the assigned areas (i.e., valuing both the objective and the ambiguous information). Following this notion, research comparing decision-making models in humans has shown a selectivity of the parietal cortex in encoding expected utility (i.e., the weight reward given by the subjective probability as expressed in Prospect Theory (?, ?)). Recent non-human primate evidence points out that parietal neurons encode the possible reduction of the uncertainty rather than the reward magnitude associated with the selected option (?, ?). Accordingly, our results did not show reward modulation in parietal areas. Thus, the parietal cortex seems to sense the predictability of the reward by differentiating information that is known from information that is not known.

Although our experiential approach depicted a specificity computation for the parietal cortex, studies in humans have shown contradictory results on the role of this area during decision-making under uncertain conditions. On the one hand, a potential causal role has been highlighted by patients with posterior parietal lesions who failed to adjust their decision to the probability of winning as patients with frontal lesions did (?, ?). On the other hand, parietal activity has been related to a surprise signal with a general effect of cognitive reallocation, for example, slowing reaction time, but not with a value-update process (?, ?). Other studies have reported a correlation between parietal activity and value processing only in specific demanding circumstances, for example, time pressure (?, ?). Parietal activity has also been correlated with the belief update, reducing the degree of ambiguity rather than value update (?, ?). In this context, our results support a causal engagement of the parietal cortex in decision-making under uncertain circumstances, as parietal interference by TMS affected a particular computation related to the management of ambiguity. Additionally, parietal suppression reduced the signal related to prediction error associated with ambiguous probabilities in the lateral prefrontal cortex. Since there is no learning in our experimental task, we cannot rule out if this activity is just a surprise signal related to expectation violation or has a role in value updating and learning. Nevertheless, since the observed behavioral modulation was associated with the accumulative effect of parietal inhibition, we expect this signal to participate in the learning process. However, the latter interpretation has to be explored with additional experimental data.

Under ambiguity, the parietal activation can also be interpreted as sensing the necessity to reduce uncertainty throughout learning, valuing, and categorizing. Thus, interrupting parietal activity could impair categorization processing, generating more straightforward decision rules. Recent research in mice has evidenced a causal role for the parietal cortex in new, but not well-learned, sensory stimuli categorization (?, ?). The parietal cortex takes part in learning and categorization processes before new stimuli have been incorporated into existing categories (?, ?). Considering that our experimental task forces participants to choose based on ambiguous stimuli, the possibility of learning a categorization in which they can incorporate a not well-known stimulus is considerably reduced. The correlation between parietal cortex activity and the degree of ambiguity in the decision revealed by our outcomes might be associated with a process to reduce the uncertainty that an ambiguous stimulus evokes. Thus, parietal activity may play a role in using previous knowledge and experience in categorical choices (?, ?, ?). Thus, the effect of parietal TMS perturbation could be interpreted as using a simpler heuristic with less categorization processing.

That is, for instance, simply dividing the hidden area of our task in half rather than making a more profound calculation. Heuristics are crucial in complex situations because they are simplified decision rules that help individuals deal with problems requiring high cognitive investment (?, ?, ?). Compared with younger adults, older adults show different parietal activity when faced with a decision under uncertainty probability associated with another heuristic (?, ?). Comparative studies indicate that nonhuman primates show ambiguity aversion as adult humans, revealing that this situation entails a high cognitive cost (?, ?, ?). Interestingly, most primates species use simple heuristics to face ambiguous decisions, and only great apes consider the ambiguity of the information in the decision process (?, ?). In accordance, researchers in developmental neuroscience have shown that children do not show ambiguity aversion (?, ?). A recent study shows that the IPS participates in implementing complex heuristics in sequential decision-making tasks (?, ?). In the light of our current results, the interference of the parietal cortex can be interpreted here as preventing the use of more complex calculations for managing ambiguity.

Considering the preceding evidence, the correlation between parietal activity and the degree of uncertainty can also reflect a high cognitive demand. Indeed, previous findings have shown that regardless of sensory properties of the stimuli, parietal activity has been largely related to numeric magnitude (?, ?, ?). The IPS has been associated with several numerical and spatial operations in humans, including arithmetic calculations and spatial rotation (?, ?). Thus, it seems that the IPS is sensitive to processing and manipulating various magnitudes, including abstract numbers, space, and time (?, ?, ?). In our results, the interference of both the PPC and the IPS regions operates on a specific parameter related to the management of ambiguity in the computational model, with no evidence of bias in choice laterality and independent of other proxies of difficulty as reaction time. The preceding is important since the right IPS has been related to spatial attention (?, ?) and that non-human primate research has linked value modulation to a specific receptive field in parietal regions. According to fMRI research, parietal activity during decision-making under uncertainty is not influenced by general attentional load (?, ?). In this context, parietal activity seems to be better understood as a specific computation (or complex heuristic implementation) rather than a general cognitive load.

During outcome evaluation, we report lateral prefrontal activity related to expectation violation based on the probability assigned in our task to the hidden (ambiguous) area. Prefrontal theta activity has a widely studied role in cognitive control and working memory (?, ?, ?, ?, ?). Extensive research in non-

human primates has linked the lateral prefrontal cortex with working memory processes (?, ?, ?). In this context, the lateral prefrontal theta activity that correlates with prediction errors has been postulated as a mechanism to update values in working memory for further behavioral adaptation (?, ?). In other words, this activity is related to cognitive control by updating the probability of occurrence of a conflictive event (?, ?, ?, ?). Prior evidence showed that activity in the PPC sustains effective connectivity with the lateral prefrontal cortex after a decision in ambiguous perceptual decision-making, and such activity biases follow decision making (?, ?). fMRI and EEG studies have associated the lateral prefrontal cortex with unexpected outcomes. For example, IFG activity correlates with the likelihood that an odd event is related to a change of the environment, or, in other terms, the unexpected uncertainty of the event (?, ?). Research using the EEG technique has demonstrated that frontal theta activity correlates with the uncertainty and unexpectedness of an event (?, ?, ?), and that it is associated with future exploration rather than exploitation strategies (?, ?). fMRI studies have yielded similar results. While the rostral prefrontal cortex activity correlates with a direct exploratory approach, the lateral prefrontal cortex correlates with a random exploratory strategy after an unexpected event (?, ?, ?). Interestingly, a similar dissociation has been found for the neural correlates of uncertainty. While the rostral frontal activity correlates with the difference of the uncertainty between options, lateral prefrontal activity (quite similar to that found in our fMRI and EEG experiments, depicted in Figure 5c) correlates with the total uncertainty of the options during decision making (?, ?). Thus, the activity related to prediction error given by the ambiguous information could be interpreted as a mechanism to contrast and update the uncertainty of the chosen event. Nonetheless, due to the lack of explicit learning in our experimental design, further empirical research must test this interpretation.

In summary, here we took advantage of the sequential use of fMRI and TMS-EES studies to localize and interfere with model-derived signals related to the use of ambiguous probabilities to provide causation. Our results demonstrate a causal implication of the parietal cortex in managing ambiguity during decision-making, assigning ambiguous probabilities to neural signals to this brain area. Additionally, we tested if the localized perturbation in the parietal cortex spreads through the cortex and alters neural processing in remote areas. Specifically, we demonstrated a decrease in the signal related to violation expectation in the lateral prefrontal cortex once participants evaluated the outcome of their decisions. Therefore, the evidence provided here contributes to generating deep insight into the cognitive and neural mechanisms underlying decision-making in situations of ambiguity. Notably, difficulties dealing with uncertainty or ambiguity

commonly result in anxiety (Stark et al., 2021). Hence, the mechanism we identified here could become a potential target for further studies in several neuropsychiatric symptoms that have been associated with the perception and the computation of uncertainty, such as Autism Spectrum Disorder (Stark et al., 2021).

2.4 Materials and Method

2.4.1 Participants

Sixty-six healthy, Spanish-speaking participants between the ages of 18 and 35 participated in the experimental protocol approved by the Ethics Committee of the Universidad del Desarrollo, Chile. Thirty-nine participants took part in the fMRI session, of which 27 participated in the EEG-TMS session. All had normal or corrected to normal vision, no color vision impairment, no history of neurological disease, and no current psychiatric diagnosis or psychotropic prescriptions. All participants gave informed consent. Experiments were conducted in the Social Neuroscience and Neuromodulation Laboratory at the Centro de Investigación en Complejidad Social (neuroCICS) at the Universidad del Desarrollo and the Unidad de Imágenes Cuantitativas Avanzadas (UNICA) at the Clínica Alemana de Santiago.

2.4.2 Task

All participants solved the probabilistic decision-making (PDM) task (Billeke et al., 2020) in which they had to decide between two probabilistic rewarded options. Each option was represented by the color of a bar (on each side of the screen) and associated with the probability of being finally selected, represented by the length of a colored bar placed in the center of the screen; and a reward, represented by a number placed over each colored bar. The options had random, complementary probabilities and rewards. The option with the highest chance had the lowest reward and vice versa. After the participant had chosen an option (2- 6 secs), the rewarded option was indicated with either a green circle in case participants chose the rewarded option or with a red circle otherwise. Feedback presentation (red or green circle) lasted 3 secs. If the participant chose the rewarded option, he/she obtained the associated payoff. Otherwise, he/she received no money. Participants solved this task in two conditions: Risk and Ambiguity. In the former condition, participants saw the full extension of the color bar, having complete information related to the

probability distribution of the possible outcome (i.e., risk or first-order uncertainty). In the latter condition, a gray mask hid part of the extension of both bars. This mask could have a size ranging from 40% to 80%. In these cases, participants had incomplete information related to the probability distribution of the possible outcome (i.e., ambiguity or second-order uncertainty). The task was programmed and presented using Presentation Software (Neurobehavioral Systems TM).

In the fMRI experimental session, participants resolved 40 trials: 20 trials for the Risk condition and 20 trials for the Ambiguity condition, in 5-trial blocks. In the TMS-EEG experimental session, participants resolved 240 trials in 10-trials blocks per condition (Risk and ambiguity). Each participant solved 6 runs of TMS stimulations, consisting of 2 runs of 40 trials with TMS interference on the PPC (MNI x=14, y=-64, z=56), two runs of 40 trials with TMS interference at the IPS (MNI x=36, y=-46, z=56) and two runs of 40 trials with TMS interference at the vertex, as an active control condition. The order of these 6 runs was randomly selected per participant. Stimulation was applied 200 and 300 ms before the Feedback epoch with a double inhibitory pulse separated by 100 ms. The TMS target regions were calculated based on the results of the group analyses of the fMRI session.

2.4.3 Statistical analysis of the behavior

The participants' answers were analyzed with a computational cognitive approach. All computational cognitive models were fitted using prospect theory, which is based on the assumption that the expected subjective value of an option Ul (l indicates left option) is defined by the following equation.

$$U_l = v(x_l)\pi(P_{all_l}) - v(x_r)\pi(P_{all_r})$$

where v(.) represents the value function, x_l and x_r denote the potential outcome of each option associated with the left or right option, respectively. P_{all_l} and P_{all_r} are the probabilities of a gain whereas π(.)are the subjective decision weights assigned to these probabilities.

$$v(x) = x^a$$

Where a determines the concavity of the value function. To accommodate for the existence of unknown probabilities (i.e., for ambiguity condition), the probability P_{all} by which the outcome x occurs is

defined by the following equations.

$$P_{all_l} = P_{obj_l} + P_{as_l} \tag{2.1}$$

$$P_{as_l} = P_a * \tau_b * \tau_i \tag{2.2}$$

$$P_{as_r} = P_a * (1 - \tau_b) * \tau_i \tag{2.3}$$

$$\pi(P_{all}) = \frac{P_{all}^{\gamma}}{(P_{all}^{\gamma} + (1 - P_{all})^{\gamma})^{\frac{1}{\gamma}}} \tag{2.4}$$

In the equations (1) to (3), P_{obj_l}, P_{obj_r}, P_a represent the normalized (P_{obj_l} + P_{obj_r} +P_{ab} =1) length of the bar that represents the visible (objective) probability of left, right options and the hidden area (ambiguity area) respectively.

The extent by which the ambiguity area P_a is assigned to each option is modulated by two parameters: τ_i that represents the ratio of the Pa effectively assigned, and τ_b that represents the ratio by which the subject biases one of the two options. The models where τ_b was set to 0.5 involving processing of unbiased (homogeneous) assignment between options (left or right). Additionally, we explored an alternative bias parameter τ_b' influenced by the difference in the reward of each option given by the following equation:

$$\tau_b' = \begin{cases} \tau_b & \text{if } x_l \geq x_r \\ (1 - \tau_b) & \text{if } x_l < x_r \end{cases}$$

The probability of choosing the left option for a given subjective value is computed using a logistic choice rule where β_1 is an inverse temperature parameter representing the degree of stochasticity in the choice process.

$$\Theta(U_l) = \frac{1}{1 + e_1^{\beta}(U_l - \beta_0)}$$

All parameters were estimated using a Hierarchical Bayesian approach that uses the aggregated information from the entire population sample to inform and constrain the parameter estimates for each individual. The hierarchical structure contains two levels of random variation: the trial (i) and participant (s) levels. At the trial level, choices were modeled following a Bernoulli process:

$$y(s,i) \sim bern(\Theta(U_l))$$

At the participant level, the model parameters were constrained by group level hyper-parameters. The parameters were restricted to be between 0 and 1 using a Beta distribution.

$$\tau_s \sim beta(\mu_\tau * k_{\tau'}(1 - \mu_\tau) * k_\tau)$$

Where μ_τ represents the mean, and represents the dispersion of the beta distribution. The parameters at the participant level were parameterized using normal distributions. The and parameters at the participant level were also parameterized using normal distributions and restricted to positive values.

$$a_{(s)} \sim normal(\mu_a, \sigma_a)$$

$$\beta_{(s)} \sim normal(\mu_\beta, \sigma_\beta)$$

$$\gamma_{(s)} \sim normal(\mu_\gamma, \sigma_\gamma)$$

Posterior inference of the parameters in the hierarchical Bayesian models was performed via the Gibbs sampler using the Markov Chain Monte Carlo (MCMC) technique implemented in JAGS using R software. A minimum of 10,000 samples were drawn from an initial burn-in sequence, and subsequently, a total of 10,000 new samples were drawn using three chains (each chain was derived based on a different random number generator engine, using different seeds). We increase the length of burn-in sequence if the chains do not meet the criteria for convergence; see below. We applied a thinning of 10 to this sample, resulting in a final set of 3x1,000 samples for each parameter. This thinning avoids that the final samples were auto-correlated for all of the parameters of interest. We conducted Gelman-Rubin tests for each parameter to confirm the convergence of the chains. All latent variables in our models had a Gelman-Rubin statistic near to 1, which suggests that all three chains converged to the target posterior distribution. Additionally, the behavior was also analyzed using mixed-effect logistic regression assuming τ_b of 0.5 and τ_i of 1. In other words, these models do not assume any specific ambiguity computation. The selected model for the statistical analysis of the behavior in the fMRI experiments considered the probability to choose the left option as the dependent variable, and the Probability of the left option (P_{all_l} = P_{obj_l} + P_a/2), the payment or reward of the left option (Rw), and the Ambiguous probability (e.i., P_a) as independent variables (Table 1):

$$Left \sim P_{all_l} + Rw_l + P_a + P_{all_l} * P_a$$

2.4.4 Anatomical Data

All participants underwent a 3D anatomical MPRAGE T1-weighted and T2-weighted Magnetic Resonance Imaging scan on a 3T Siemens Skyra (Siemens AG, Erlangen, Germany) before (no more than 3 months) of

the TMS-EEG sessions or together with the fMRI sessions. The anatomical volume consisted of 160 sagittal slices of an isotropic voxel (1x1x1 mm), covering the whole brain. The scalp and cortical surfaces were extracted from the T1-weighted / T2-weighted corrected anatomical MRI using a pipeline available from the Human Connectome Project. Thus, a surface triangulation was obtained for each envelope (Fischl, 2012). The individual high-resolution cortical surfaces (300 000 vertices per cortical surface) were down-sampled to 5 000 vertices. Additionally a five-layer segmentation based on T1-weighted / T2-weighted corrected and T2-weighted was carried out using the algorithm implemented by the SimNIBS tool and SMP12. The cortical mesh and five-layer segmentation served as image supports for the EEG source estimation, see below.

2.4.5 Functional MRI Data

For the functional images, volumes of the entire weighted echo-planner T2* brain were acquired while the experimental task was executed (3x3x3 mm voxels). Participant volumes were coregisterd to 2-mm standard imaging using the nonlinear algorithm implemented in FSL. The BOLD signal was analyzed using different models including motion correction parameters. During decision making periods, we fitted two models, the first one included Rw , P_{obj} and P_{as} of the chosen option using the Equations 2 and 3 using τ_i estimated for each subject using the selected computational cognitive model. In figure 3 we show the P_{as} regressor that was orthogonalized to P_{obj} and normalized in order to capture a different variance than that captured by P_a regressor (using P_{obj_chosen}/ (P_{obj_chosen}+$P_{obj_unchosen}$)). Using this method, the normalized Pas is independent of P_a. Additionally, in another model we included P_{as} not normalized (and assuming τ_i = 1), that is shown in the Figure 3 as P_a (P_{as}=P_{ab}/ 2). These results are quite similar to the Pas regressor calculated with the individual τ_i and with that orthogonalized to P_{obj}. Additionally, all the models included the following control regressors: Am as a dummy regressor capturing the "state" or baseline activity that the participants had in the ambiguity condition, and the reaction-time regressor as a proxy of difficulty. For the BOLD signal during outcome evaluation (feedback) we used the following regressors of interest: Win (a dummy regressor indicating that the chosen option was rewarded), Rw(the amount of the obtained reward), uPE-P_{obj} (the unsigned prediction error of the fact to win or not to win given by the P_{obj} of the chosen option), uPE-P_{as} (the unsigned prediction error of the fact to win or not win given by the Pas of the chosen option), uPE-Rw (the unsigned prediction error of the amount of the obtained reward). All

regressors were convolved using a double gamma function.

2.4.6 EEG Recordings

We used TMS-compatible EEG equipment (BrainAmp 64 DC, BrainProducts, http://www. brainproducts.com/). EEG was continuously acquired from 64 channels (plus an acquisition reference (FCz) and a ground). TMS- compatible sintered Ag/AgCl-pin electrodes were used. The signal was band-pass filtered at DC to 1000 Hz and digitized at a sampling rate of 5000 Hz. Skin/electrode impedance was maintained below 5 kOhm. Electrode impedances were re-tested during pauses to ensure stable values throughout the experiment. The positions of the EEG electrodes were estimated using the neuronavigation system used for the TMS.

2.4.7 EEG-TMS Protocol

TMS was applied during task performance and during EEG recordings. Participants were instructed to maintain central fixation and to minimize eye blinks and other movements during the recording blocks. Double biphasic TMS pulses were delivered over the right IPS (TMSips, MNI [41, -36, 40]), the right PPC (TMSppc, MNI [14, -64, 56]) and the Vertex (TMSvertex, MNI [0, -29, 77]; see Results, Figures 3 and 4A) using a 70 mm figure-of-eight TMS coil connected to Mag and More Stimulator. A Neuronavigation system was used to identify individual stimulation points (individual structural MR scans, native space) in the nearest gray matter areas to the no-linear inverse co-registration of the individual anatomy (FSL algorithm, default parameters). TMS coil positioning and orientation with regards to brain x,y and z axes (yaw, pitch and roll) were optimized so that the electric field impacted perpendicular the target region, maximizing the induced current strength (Thut et al., 2011; Valero-Cabré et al., 2017). This approach results for all subjects with approximately an angulation in a horizontal plane (yaw) with regards to the interhemispheric fissure of 45o for the IPS and 0 o for the PPC and the vertex. For each trial and for both tasks, two consecutive single TMS pulses were delivered before the feedback presentation (-300 and -200 ms pre-stimulus onset) with an interpulse interval of 100 ms in order to interfere with target activity with a 100-200 ms window that has been used in prior work (Chica et al., 2011; Oshio et al., 2010) and has been demonstrated to inhibit motor potential (Chen et al., 1997). TMS intensity was fixed at 120% of individual

resting motor threshold (TMS intensity ranging from 54% to 78% of the maximum machine power and a mean of 63%). Each TMS session included six runs. In each run, 40 two-pulse TMS bursts were delivered trial by trial, leading to 80 pulses per run over a block duration of about 11 min. Pauses for a minimum of 5 minutes of duration separated each run. Each TMS-EEG experiment thus contained a total of 480 active TMS pulses (including those delivered at the vertex). Two 5-min EEG resting-state recordings were performed before and after the six blocks. The duration of the experiment was around 180 minutes: one hour for setting the EEG electrodes at stable and adequate impedances, one and half hours of recordings, and 30 minutes for the electrode MRI localization and experiment finalization. The TMS protocol respected at all times past and current safety recommendations regarding stimulation parameters (intensity, number of pulses, and ethical requirements (Rossi et al., 2009, 2021; Rossini et al., 2015)).

2.4.8 EEG Pre-processing and TMS Artifact Removal

Preprocessing were performed in multiple steps. We first detected the slow decay component of the TMS artifact. To this end, we segmented 1-second windows containing TMS pulses, automatically detected a period starting 10 ms pre to 20 ms post to the respective TMS peak, and removed this from the signal. We applied an Independent Component Analysis (ICA) to this signal using the Runica algorithm provided by the EEGLAB toolbox (https://sccn.ucsd.edu/eeglab/). Thus, we looked for a stereotype component with local bipolar distribution over TMS site pulse. In the second step, we segmented the raw signal in the time-widows of analysis (-1.5 seconds to 2 seconds after feedback onset). Then, we removed the segment between -10 to 30 ms around TMS peak and replaced it by an inverse-distance weighted interpolation [Y $=sum(X/D^3)/sum(1/D^3)$] plus a Gaussian noise with the standard deviation extracted to a reference period set to be 55 to -15 ms before the respective first TMS peak of the double pulse and 0 of the mean. Then, we removed the TMS ICA components computed in the first step. This procedure effectively removes the direct (non-physiological) and other TMS artifacts (e.g., TMS locked artifacts at electrodes directly in contact with the TMS coil) without introducing discontinuities, important for the later time-frequency analysis (Albouy et al., 2017; Thut et al., 2011). Following these steps, we down-sampled EEG data to 1000 Hz and used a preprocessing pipeline developed for prior work (?, ?, ?, ?, ?). The EEG data was 0.1–45 Hz band-pass filtered. Artifacts were first automatically detected using a threshold of 150 V and a power spectrum greater than two std. dev. for more than 10% of the frequency spectrum (0.5 to 40 Hz). Blinking

was extracted from the signal by means of ICA. Trials that included artifacts detected by visual inspection of the signal were eliminated. The mean of artifact-free trials was 229 out of 240, ranges: [182 - 240]. Finally, the signal was re-referenced offline to the average of all electrodes for the subsequent analyses.

Time-frequency (TF) distributions were obtained by means of the wavelet transform in a time window between -1.5 and 2s around feedback onset. To this end, the signal x(t) was convolved with a complex Morlet's wavelet function. Wavelets were normalized, and thus the width of each wavelet function was chosen to be five cycles. Thus, we obtained the phase and amplitude per each temporal bin (in steps of 10ms) and frequency (from 1 to 40Hz in steps of 1Hz). For all power spectrum analyses, we used the dB of power related to a baseline during the fixation phase (at the beginning of the experiments). To avoid edge artifacts, only the period between -0.5 to 1s over the segmented signals was used for additional analyses. We calculated general linear models for each subject based on single-trial wavelet transform (first level-analysis). We used the same regressor as in the fMRI feedback model, namely Win, Rw, uPE-Pobj, uPE-Pobj, uPE-Rw, Am, and a regressor for each TMS stimulation (TMSips, TMSppc) and the interaction between the TMS regresor with the preceding regressors. Thus, per each regressor and subject, we obtained a 3D matrix (time, frequency, electrode), which we used in the second-level analysis. For the analyses of the frontal electrodes of interest, the 3D matrix was meant in the electrode dimension including only the selected ones (CFz, Fz, AFz). For the whole scalp analysis, the entire 3D matrix was used. For both cases, we then compared each bin of these matrices across participants. We explored for consistent modulations in the same condition. For this, we used the Wilcoxon signed sum test, evaluating whether the mean is different from zero. All comparisons were corrected for multiple comparisons using a cluster based permutation test (see below, (Maris and Oostenveld, 2007) or false discovery rate (FDR) for a priori selection of a frequency-time window of interest).

2.4.9 Cluster-based Permutation test

In order to correct for multiple comparisons in the time-frequency analysis, we carried out a permutation test (Maris and Oostenveld, 2007). Here, clusters of significant areas were defined by pooling neighboring sites that showed the same effect ($p<0.05$ in the statistical test carried out in sites of either the time-frequency chart or the sources, e.g., Wilcoxon test). The cluster-level statistics were computed as the sum of the statistics of all sites within the corresponding cluster. We evaluated the cluster-level significance

under the permutation distribution of the cluster that had the largest cluster-level statistics. The permutation distribution was obtained by randomly permuting the original data. Specifically, for each subject, we carried out null models, where the same structure of the original model was preserved, but the regressor to be tested was permuted. After each permutation, the original statistical test was computed (e.g., Wilcoxon), and the cluster-level statistics of the largest resulting cluster were used for the permutation distribution. After 5000 permutations, the cluster-level significance of each observed cluster was estimated as the proportion of elements of the permutation distribution greater than the cluster-level statistics of the corresponding cluster.

2.4.10 EEG Source Estimation

The neural current density time series at each brain location was estimated by applying a minimum norm estimate inverse solution LORETA algorithm with unconstrained dipole orientations in single-trials per condition and per subject, implemented in Brainstorm. A tessellated cortical mesh for individual anatomy was used as a brain model to estimate the current source distribution. We defined 3x5000 sources constrained to the segmented cortical surface (3 orthogonal sources at each spatial location), and computed a five-layer continuous Galerkin finite element conductivity model (FEM, as implemented in DUneuro software, (Piastra et al., 2018)) and the physical forward model. To estimate cortical activity at the cortical sources, the recorded raw EEG time series at the electrodes was multiplied by the inverse operator to yield the estimated source current, as a function of time, at the cortical surface. Since this is a linear transformation, it does not modify the frequencies of the underlying sources. It is therefore possible to undertake time-frequency analysis on the source space directly. In this source space, we computed frequency decomposition using the Wavelets transform. In order to minimize the possibility of erroneous results we only present source estimations if there are both statistically significant differences at the electrode level and the differences at the source levels survive a multiple comparison correction (FDR $q<0.05$).

-	Estimate std.	Error	Z value	Pr($>\|z\|$)
(Intercept)	-9.03***	1.2	-7.3	2e-13
P_{all_1}	12.5***	1.4	8.6	2e-16
Reward (Rw_l)	6.1***	1.2	5.0	4e-7
P_a	8.4**	1.7	4.9	8e-7
$P_{all_1} : P_a$	-14.7***	2.1	-6.9	4e-12
Rw:P_a	-2.6	1.5	-1.7	0.08

Table 2.1: **Behavioral results of Logic Mixed Model.** Dependent Variable: choice left option 38 subject, subject as a group factor for random effect.

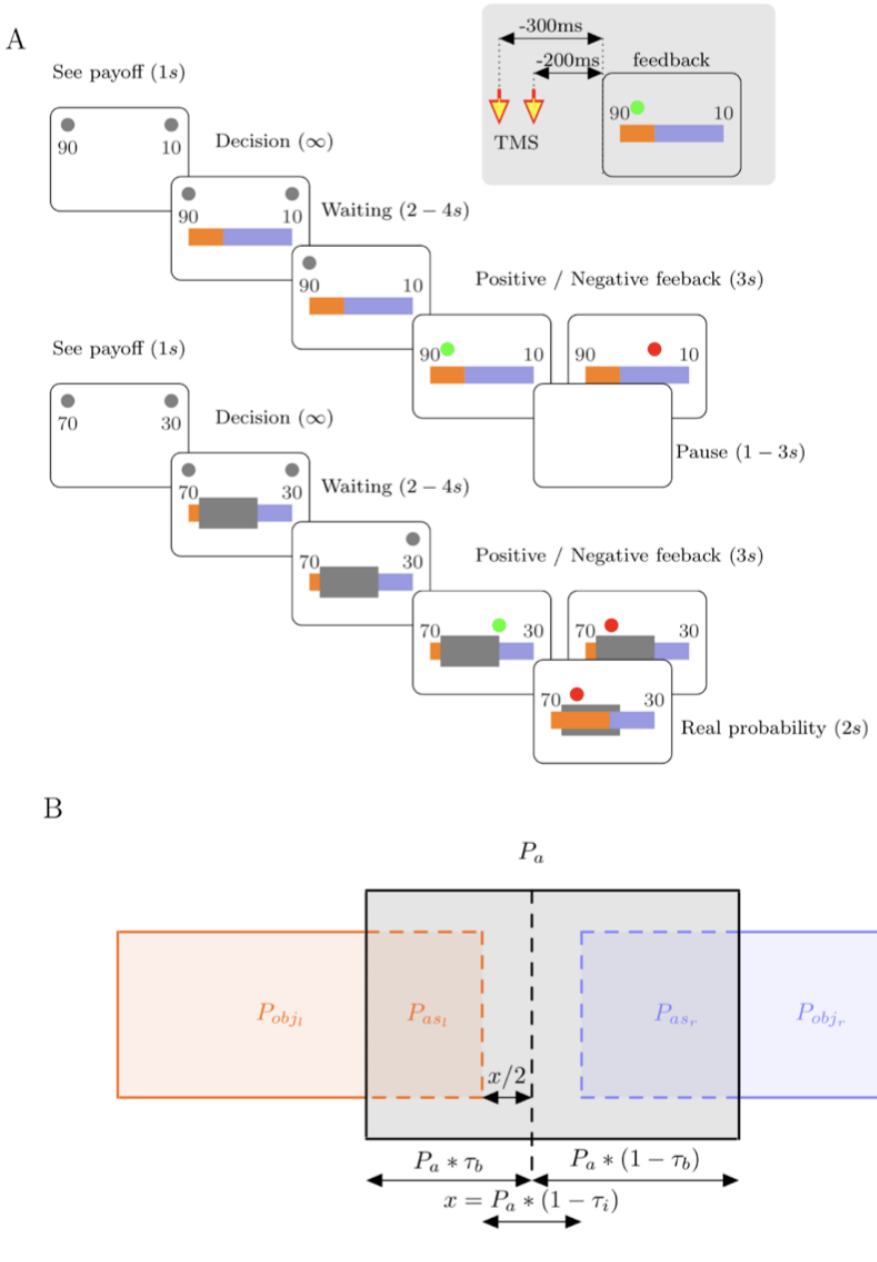

Figure 2.1: **A.** Probability Decision-Making Task. Participants had to make a decision between two options (left or right option). Each option had an associated reward indicated by a number. After a decision was made with a variable waiting time, the feedback was provided. A green circle indicates that the participants win, whereas a red circle signals that they did not. In the condition with ambiguity (bottom panel), a grey mask partially hides the color-bars extension in the division of them. In the TMS-EEG session, a double TMS pulse is delivered -300 and -200 ms before feedback presentation as represented in the gray rectangle over the superior right corner. **B.** Schematic representation of the objective probabilities (P_{obj}) and assigned probabilities (P_{as}), and the relationship among the ambiguity probability (P_a) and the model parameters, τ_i and τ_b (see the Results and Materials and Method sections for details).

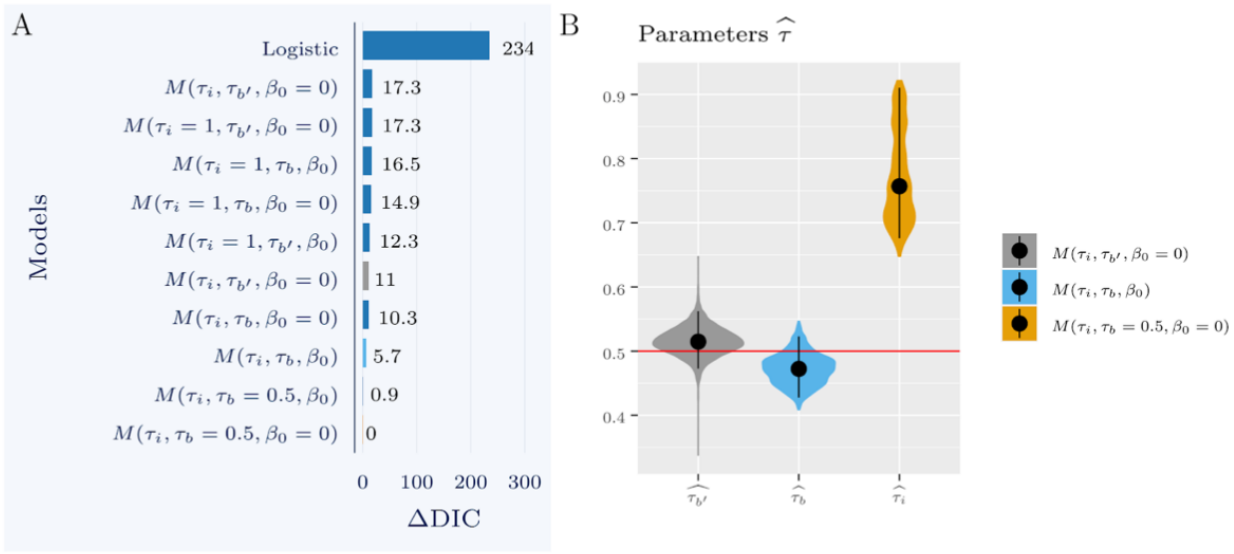

Figure 2.2: **Comparison among models and parameters. A.** Comparison of the model adjustment assessed by means of the Deviance Information Criterion (DIC). The selected model M(τ_b=0.5, τ_i, β_0=0) was used as a reference. **B.** Different parameters were estimated from the best-fitted models that considered the corresponding parameter as a free parameter. The color indicates the models from which each parameter was readout of (see main text for further details). Filled black dots represent the medians and black lines the 95% high-density intervals of the posterior distributions. The colored areas represent the complete posterior distribution. The red horizontal line indicates 0.5 as a reference to non-significant bias for τ_b and $\tau_{b'}$ parameters.

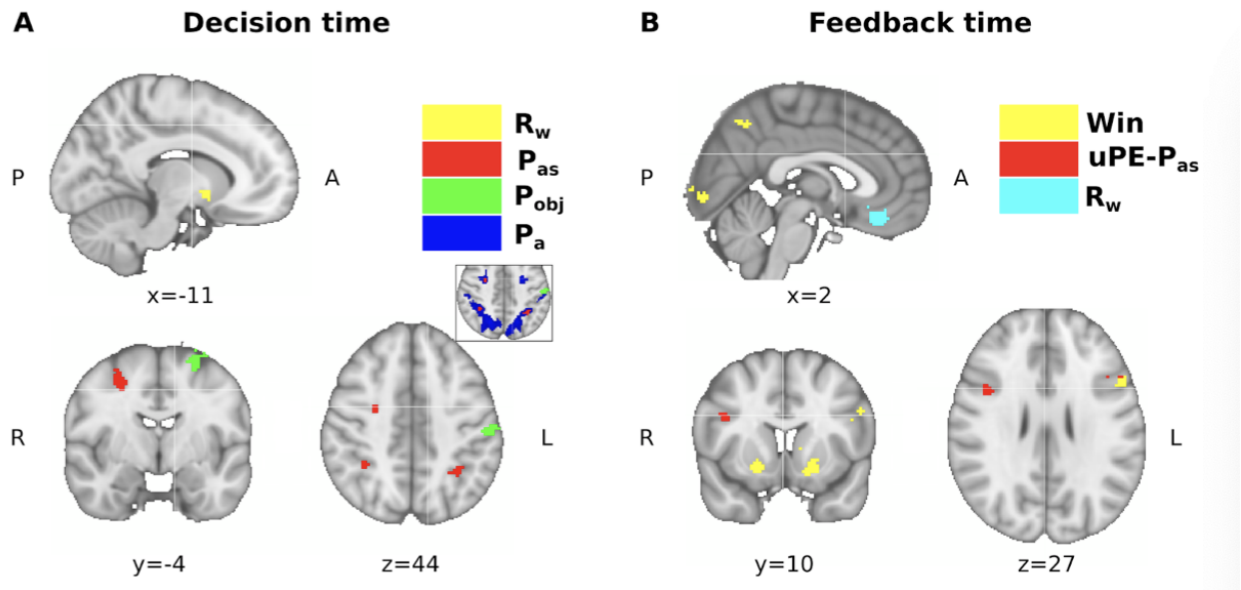

Figure 2.3: **. Brain activity during decision-making and feedback. A.** Brain activity during the decision-making period. Reward magnitude (Rw, yellow) of the chosen option is related to the activity in the ventral striatum (Cluster Threshold Detection (CTD) Z = 3.1, cluster corrected p-value <3e-8). Objective probability (P_{obj}, green) correlated with the activity in the FEF and in the IPS (CTD z=3.1, cluster corrected p-value p <0.0003). Assigned probability (P_{as}, red) correlated with bilateral activity in the IPS and in the right FEF (CTD z=3.1, cluster corrected p-value p <0.036). **B.** Brain activity during feedback. The fact of winning (Win, yellow) correlated with ventral striatum activity (CTD Z = 3.1, cluster corrected p-value <1e-5), the obtained reward (Rw, cyan) magnitude correlated with ventromedial prefrontal cortex activity (CTD Z = 3.1, cluster corrected p-value <1.e-6), and the unsigned probability prediction from assigned probability (uPE-P_{as}, red) correlated with activity in the bilateral IFG (CTD Z = 3.1, cluster corrected p-value <0.003). See also Supplementary Table 2.

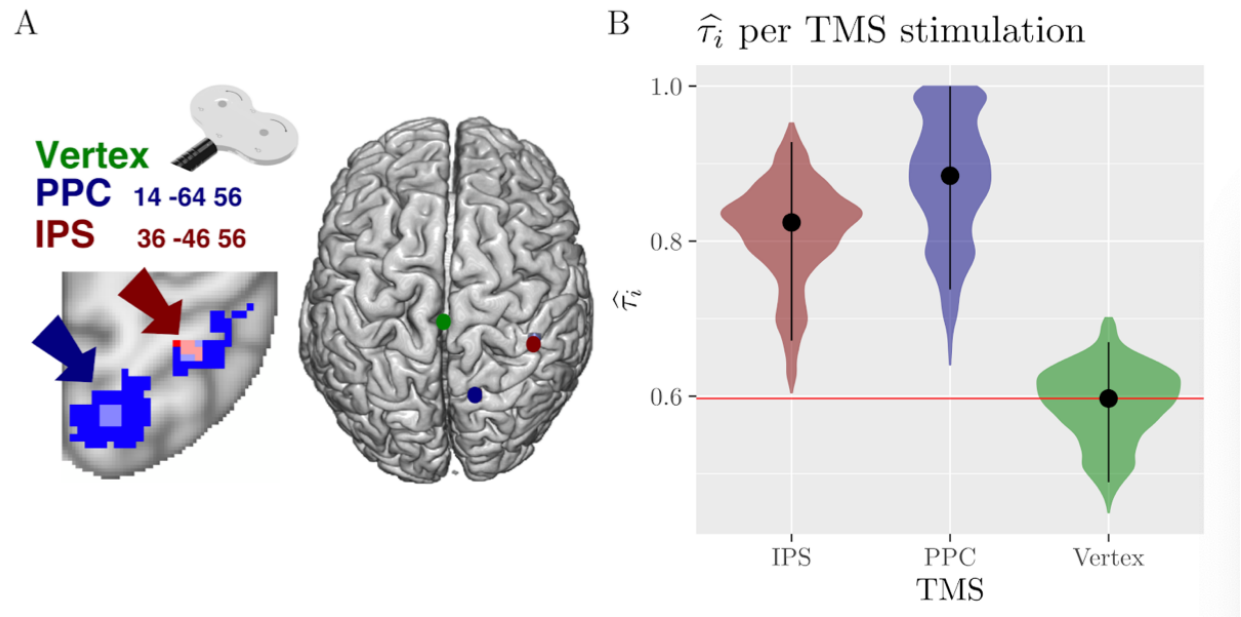

Figure 2.4: **. Behavioral result of interleaved EEG-TMS experiments. A.** Target areas for TMS stimulation and their relationship with BOLD activity in the decision-making period correlated with P_{as} (red) and P_a(blue). **B.** τ_i parameters estimated from the different TMS site (right PPC x=14, y=-64, z=56; right IPS x=36, y=-46, z=56 and Scalp Vertex). Black dots represent the means, and black lines the 95% high-density intervals of the posterior distributions. The colored areas represent the complete posterior distribution. The red line indicates the mean of the posterior distribution of the estimated τ_i parameter from vertex stimulation

.

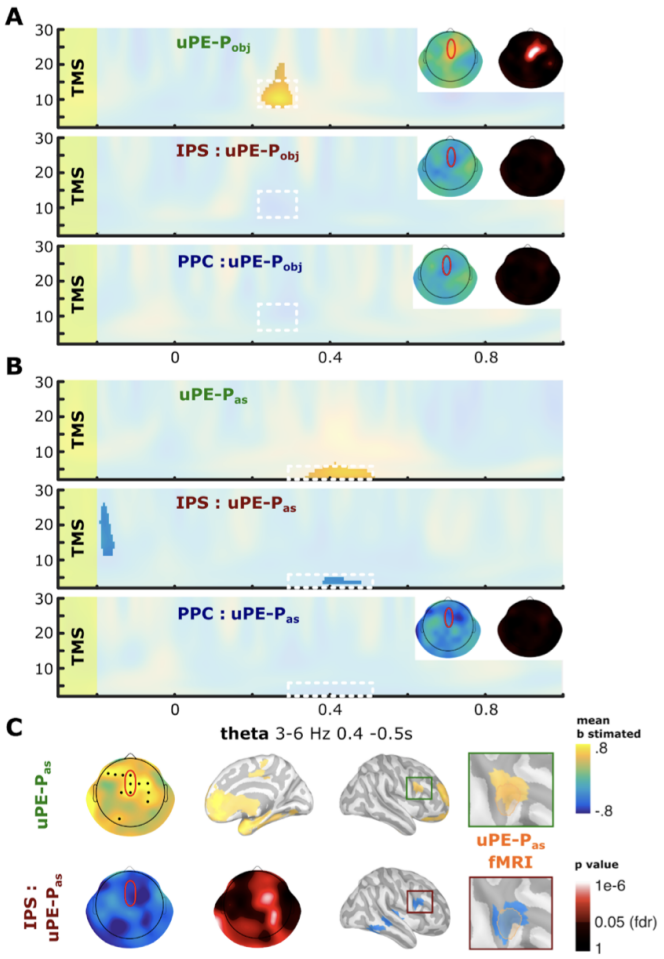

Figure 2.5: **Oscillatory brain activity in frontal electrodes associated with unsigned prediction error (uPE) during feedback. A.** Time-frequency chart in frontal electrodes (empty red oval in the topographic plot) for the correlation between oscillatory power and unsigned prediction error given by objective probability (uPE-P_{obj}) for Vertex TMS stimulation, and for the difference between vertex TMS and the IPS (IPS:uPE-P_{obj}) and the PPC (PPC:uPE-P_{obj}) TMS stimulation conditions. **B.** Time-frequency chart in frontal electrodes (empty red oval in the topographic plot) for the correlation between oscillatory power and unsigned prediction error given by assigned probability (uPE-P_{as}) for Vertex TMS stimulation, and for the difference between vertex and the IPS (IPS:uPE-P_{as}) and the PPC (PPC:uPE-P_{as}) TMS stimulation. **A-B.** The highlighted areas indicate time-frequency epochs showing significant modulation (without a prior, whole scalp/frequency/time analysis, cluster-based permutation test, p<0.001, CTD: p <0.05 Wilcoxon test). Scalp topographies show oscillatory activity in the time windows indicated in the white intermittent line rectangles for each time-frequency chart (Alpha for uPE-P_{obj}, 9-15 Hz, 0.2-0.3 s post feedback, and theta for uPE-P_{att}, 3-6 Hz, 0.3 - 0.5 post feedback). Right scalp topographies show significant electrodes in selected time-frequency windows (FDR q <0.05). **C.** Scalp topographies and sources estimation for theta activity correlated with uPE-P_{as} and IPS:uPE-P_{as}. Sources that survive multiple comparison corrections are shown (FDR q <0.05). The highlighted areas (green and red inserts) represent the coincident areas for EEG source-estimation and BOLD activity for the fMRI experiment. All source results are shown in a high-resolution mesh only for visualization purposes.

References

Angela, J. Y., & Dayan, P. (2005). Uncertainty, neuromodulation, and attention. *Neuron*, *46*(4), 681–692.

Aston-Jones, G., & Cohen, J. D. (2005). Adaptive gain and the role of the locus coeruleus–norepinephrine system in optimal performance. *Journal of Comparative Neurology*, *493*(1), 99–110.

Bernat, E. M., Nelson, L. D., Holroyd, C. B., Gehring, W. J., & Patrick, C. J. (2008). Separating cognitive processes with principal components analysis of eeg time-frequency distributions. In *Advanced signal processing algorithms, architectures, and implementations xviii* (Vol. 7074, pp. 240–249).

Billeke, P., Ossandon, T., Perrone-Bertolotti, M., Kahane, P., Bastin, J., Jerbi, K., … Fuentealba, P. (2020). Human anterior insula encodes performance feedback and relays prediction error to the medial prefrontal cortex. *Cerebral Cortex*, *30*(7), 4011–4025.

Bland, A. R., et al. (2012). Different varieties of uncertainty in human decision-making. *Frontiers in neuroscience*, *6*, 85.

Boorman, E. D., Rushworth, M. F., & Behrens, T. E. (2013). Ventromedial prefrontal and anterior cingulate cortex adopt choice and default reference frames during sequential multi-alternative choice. *Journal of Neuroscience*, *33*(6), 2242–2253.

Cavanagh, J. F., Cohen, M. X., & Allen, J. J. (2009). Prelude to and resolution of an error: Eeg phase synchrony reveals cognitive control dynamics during action monitoring. *Journal of Neuroscience*, *29*(1), 98–105.

Clark, A. (2013). Whatever next? predictive brains, situated agents, and the future of cognitive science. *Behavioral and brain sciences*, *36*(3), 181–204.

Cohen, M. X., & Ranganath, C. (2007). Reinforcement learning signals predict future decisions. *Journal of Neuroscience*, *27*(2), 371–378.

D'Ardenne, K., McClure, S. M., Nystrom, L. E., & Cohen, J. D. (2008). Bold responses reflecting dopaminergic signals in the human ventral tegmental area. *Science*, *319*(5867), 1264–1267.

Dayan, P., & Jyu, A. (2003). Uncertainty and learning. *IETE Journal of Research*, *49*(2-3), 171–181.

Dayan, P., & Yu, A. J. (2006). Phasic norepinephrine: a neural interrupt signal for unexpected events. *Network: Computation in Neural Systems*, *17*(4), 335–350.

Diederen, K. M., Spencer, T., Vestergaard, M. D., Fletcher, P. C., & Schultz, W. (2016). Adaptive prediction error coding in the human midbrain and striatum facilitates behavioral adaptation and learning efficiency. *Neuron*, *90*(5), 1127–1138.

Domenech, P., Redouté, J., Koechlin, E., & Dreher, J.-C. (2018). The neuro-computational architecture of value-based selection in the human brain. *Cerebral Cortex*, *28*(2), 585–601.

Doya, K. (2008). Modulators of decision making. *Nature neuroscience*, *11*(4), 410–416.

Falkenstein, M. (1990). Effects of errors in choice reaction tasks on the erp under focused and divided attention. *Psychophysiological brain research*.

Friston, K. (2012). The history of the future of the bayesian brain. *NeuroImage*, *62*(2), 1230–1233.

Gehring, W. J., Coles, M. G., Meyer, D. E., & Donchin, E. (1990). The error-related negativity: an event-related brain potential accompanying errors. *Psychophysiology*, *27*(4), S34.

Glimcher, P. W., & Fehr, E. (2013). *Neuroeconomics: Decision making and the brain*. Academic Press.

Gueguen, M., Lopez-Persem, A., Billeke, P., Lachaux, J.-P., Rheims, S., Kahane, P., … Bastin, J. (2021). Anatomical dissociation of intracerebral signals for reward and punishment prediction errors in humans. *Nature communications*, *12*(1), 1–12.

Huettel, S. A., Song, A. W., & McCarthy, G. (2005). Decisions under uncertainty: probabilistic context influences activation of prefrontal and parietal cortices. *Journal of Neuroscience*, *25*(13), 3304–3311.

Kable, J. W., & Glimcher, P. W. (2009). The neurobiology of decision: consensus and controversy. *Neuron*, *63*(6), 733–745.

Kahneman, D., & Tversky, A. (2013). Prospect theory: An analysis of decision under risk. In *Handbook of the fundamentals of financial decision making: Part i* (pp. 99–127). World Scientific.

Knill, D. C., & Pouget, A. (2004). The bayesian brain: the role of uncertainty in neural coding and computation. *TRENDS in Neurosciences*, *27*(12), 712–719.

Knutson, B., & Wimmer, G. E. (2007). Splitting the difference: how does the brain code reward episodes? *Annals of the New York Academy of Sciences*, *1104*(1), 54–69.

Ma, W. J., & Jazayeri, M. (2014). Neural coding of uncertainty and probability. *Annual review of neuroscience*, *37*, 205–220.

Marco-Pallares, J., Cucurell, D., Cunillera, T., García, R., Andrés-Pueyo, A., Münte, T. F., & Rodríguez-Fornells, A. (2008). Human oscillatory activity associated to reward processing in a gambling task. *Neuropsychologia*, *46*(1), 241–248.

Miltner, W. H., Braun, C. H., & Coles, M. G. (1997). Event-related brain potentials following incorrect feedback in a time-estimation task: evidence for a "generic" neural system for error detection. *Journal of cognitive neuroscience*, *9*(6), 788–798.

Montague, P. R., Dayan, P., & Sejnowski, T. J. (1996). A framework for mesencephalic dopamine systems based on predictive hebbian learning. *Journal of neuroscience*, *16*(5), 1936–1947.

Polanía, R., Krajbich, I., Grueschow, M., & Ruff, C. C. (2014). Neural oscillations and synchronization differentially support evidence accumulation in perceptual and value-based decision making. *Neuron*, *82*(3), 709–720.

Polezzi, D., Sartori, G., Rumiati, R., Vidotto, G., & Daum, I. (2010). Brain correlates of risky decision-making. *Neuroimage*, *49*(2), 1886–1894.

Quirk, G. J., & Mueller, D. (2008). Neural mechanisms of extinction learning and retrieval. *Neuropsychopharmacology*, *33*(1), 56–72.

Rangel, A., Camerer, C., & Montague, P. R. (2008). A framework for studying the neurobiology of value-based decision making. *Nature reviews neuroscience*, *9*(7), 545–556.

Sales, A. C., Friston, K. J., Jones, M. W., Pickering, A. E., & Moran, R. J. (2019). Locus coeruleus tracking of prediction errors optimises cognitive flexibility: An active inference model. *PLoS computational biology*, *15*(1), e1006267.

Schultz, W. (2016). Dopamine reward prediction-error signalling: a two-component response.

Nature reviews neuroscience, *17*(3), 183–195.

Schultz, W., Apicella, P., & Ljungberg, T. (1993). Responses of monkey dopamine neurons to reward and conditioned stimuli during successive steps of learning a delayed response task. *Journal of neuroscience*, *13*(3), 900–913.

Sutton, R. S., & Barto, A. G. (2018). *Reinforcement learning: An introduction*. MIT press.

Trujillo, L. T., & Allen, J. J. (2007). Theta eeg dynamics of the error-related negativity. *Clinical Neurophysiology*, *118*(3), 645–668.

Yeung, N., & Sanfey, A. G. (2004). Independent coding of reward magnitude and valence in the human brain. *Journal of Neuroscience*, *24*(28), 6258–6264.

Zhang, S., Hu, S., Chao, H. H., & Li, C.-S. R. (2016). Resting-state functional connectivity of the locus coeruleus in humans: in comparison with the ventral tegmental area/substantia nigra pars compacta and the effects of age. *Cerebral Cortex*, *26*(8), 3413–3427.

Chapter 3

Parietal cortex participates in the modulation of learning rate in highly uncertain volatile contexts in human decision-making

Gabriela Valdebenito-Oyarzo[1], María Paz Martinez-Molina[1], Nicolás Ferrer[1], Josefina Larraín-Valenzuela[1], Francisco Zamorano[1,2], Ximena Stecher[2], Rafael Polania[3] and Pablo Billeke[1 1]

[1]Laboratory of Social Neuroscience and Neuromodulation, Centre for Research in Social Complexity, (neuroCICS), Faculty of Government, Universidad del Desarrollo, Santiago, Chile.

[2]Department of Imaging, Clinica Alemana De Santiago, Chile.

[3] Decision Neuroscience Lab, Department of Health Sciences and Technology, ETH Zurich, Zurich, Switzerland.

[1]CONTACT Gabriela Valdebenito-Oyarzo Email: gvaldebenitoo@udd.cl

Highlights

(i) In contexts of volatility the learning rate is higher than in contexts of stable uncertainty.

(ii) In contexts of high volatile uncertainty there is an activation of the parietal cortex weighted by the rate of learning during feedback.

Abstract

The decision-making process in volatile contexts destabilises the learning process of the probabilistic distribution of options, so updating the learning rate is crucial for task success. The parietal cortex is involved in uncertainty computation, but its specific role is not known. We tested under fMRI a decision making task in the context of stable uncertainty and volatility involving a learning process. We tested the hypothesis that the parietal cortex is involved in modulating the rate of probability learning in volatile contexts. We found that in volatility contexts the learning rate is higher than in stable uncertainty contexts. In the volatility condition with high uncertainty, we observed an increase in the activity of the parietal cortex in the feedback period considering the update of the learning rate of each trial. These results contribute to explain the role of the parietal cortex in the uncertain decision making process.

Keywords: Decision-making; Uncertainty, Volatile; Learning Rate; Parietal Cortex

2

3.1 Introduction

Volatility is a type of uncertainty where contingencies change and subjects must adapt or be cognitively flexible to process uncertainty. Changing environments destabilise the construction of option value so that the correct integration of stimulus-action-consequence is essential for success in the process. Adapting to environmental or contingency changes requires updating knowledge of the probabilistic distribution of options (Yaple and Yu, 2019). Los cambios de contingencia conducen a la exploración, therefore

uncertainty-driven exploration is a potentially important facet of decision-making and adaptive behavior (?, ?). Changes in the probability of occurrence involve adaptive learning of Prediction Error (PE), evidence has shown that the midbrain and ventral striatum are involved in this processing (Diederen et al., 2016). In reversal learning tasks, it has been observed that reversal error (error related to the use of the same strategy after the change in probability distribution) is processed by the fronto-parietal network, which would indicate that the activity of this network may reflect an increase in adaptive control as a means of adjusting to previous errors between trials (?, ?).

Studies in volatility (or reverse learning) contexts have revealed activation of the Locus Coereleus (LC) nucleus showing that phasic activity releases the neuromodulator Noradrenaline and is thought to encode the outcome of our decisions, while in its tonic activity it would preferentially encode subsequent behavioural change ((Aston-Jones & Cohen, 2005; Angela & Dayan, 2005; Dayan & Yu, 2006; Sales et al., 2019). This tonic activity possibly leads to a further increase in the learning function in contexts of volatility, i.e. increased learning when there is a change in the belief of the known world (Dayan & Jyu, 2003). A Resting-state study demonstrates that there is a connectivity between LC with the fronto-parietal network that is usually activated in the coding tasks of choice in contexts of uncertainty, whose role is not yet clear (Zhang et al., 2016).

We hypothesise that the parietal cortex is involved in the modulation of learning in volatile contexts. We test our hypothesis by designing a decision making task in the context of stable uncertainty and volatility to assess the neurobiological activity and behavioural data associated with updating the rate of learning in these contexts.

3.2 Results

3.2.1 Behavioral Model

In our behavioural task, participants had to make a prediction by choosing one of twenty possible options. The higher the accuracy of the prediction, the higher the associated reward, and the task had a total of 8 conditions (high and low stable uncertainty, high or low volatile uncertainty, 2 false conditions, and 2 noise conditions) (see Figure 3.1). The goal was for subjects to learn through trials where an arrow shot

by an archer whose target position was unknown would land.

First, we assessed whether there was a difference between the learning rate for the stable and volatile uncertainty condition of the task by fitting a learning model for each subject. This model adjusted the prediction of each cue, based on the prediction error of the previous trial, as shown in the following equation:

$$P_{(t)} = P_{(t-1)} + \alpha + PE$$

$$PE = F_{(t-1)} - P_{(t-1)}$$

$$\alpha = \alpha_U + \alpha_V$$

Where P is the prediction, t is current trial , $t-1$ is preceding trial, α is learning rate, PE is the Prediction Error and F is the feedback (the correct answer). Alpha was obtained from the sum of the learning rate of each condition where α_U corresponds to learning rate of stable uncertainty condition and α_V is the learning rate of volatile condition.

The first behavioral results demonstrated a less learning rate in the uncertainty condition (α_U=-0.0813, p value= 0.0210) and a higher learning rate for the volatility condition ($alpha$= 0.1531, p value=0.0210).

Considering that there are differences between the learning rate of stable uncertainty and volatile uncertainty we decided to search for how the mean and standard deviation variables affect the subject's prediction in each condition. Therefore, we test a model to predict a future outcome from past experience in a dynamic environment. The algorithm defining belief adaptation was proposed by:

$$\beta(t+1) = \beta(t) + \alpha * \delta(t) \tag{3.1}$$

Were $\beta(t+1)$ represents the update of belief in (t+1), $\beta(t)$ in previous belief, $\alpha(t)$ is the learning rate that take a value between 0-1. $\delta(t)$ represent the Prediction Error (PE) of the last trial.

Given the characteristics of the experimental design, we designed a model using a hierarchical Bayesian approach that uses information from the entire population sample to inform and constrain parameter estimates for each individual. The hierarchical structure contains two levels of random variation: the trial level and the participant level. At the trial level, choices were modelled following a normal process.

Our Model 1 considering $\alpha\mu$ (mean) and 1 $\alpha\sigma$ (standar desviation).

$$SP(t) \sim N(SP\mu(t), SP\sigma(t)) \tag{3.2}$$

$SP(t)$ represents the subject's prediction or decision at trial t, $SP\mu(t)$ is the prediction of median in the trial t and $SP\sigma(t)$ is the prediction of standar desviation in trial t.

The obtainment of $SP\mu(t)$ is given by:

$$SP\mu(t) = SP\mu(t-1) + \alpha\mu * \delta\mu(t) \tag{3.3}$$

$$\delta\mu(t) = F(t-1) - SP\mu(t-1) \tag{3.4}$$

$SP\mu(t-1)$ represent the prediction of mean in previous trial, $\alpha\mu$ is the learning rate of mean and $\sigma\mu(t)$ represent the PE in trial t.

$SP\sigma(t)$ is obtein from,

$$SP\sigma(t) = SP\sigma(t-1) + \alpha\sigma * \delta\sigma(t) \tag{3.5}$$

$$\delta_{\sigma}(t) = F\sigma(t-1) - SP\sigma(t-1) \tag{3.6}$$

$$F\sigma(t-1) = \sqrt[2]{F(t-1) - F(t-2)} \tag{3.7}$$

The results show that the model has a good overall fit when analysing the data with all conditions (Table 3.1), however when this model is applied separately to each condition the fit worsens for the volatility conditions (Table 3.2 and 3.3). We tried fitting a second model that splits sigma into σ_{high} and σ_{low} given the high and low stable uncertainty task condition. The model corresponds to:

MODELO 2: $\alpha\mu$ 2 σ

$SP\mu(t)$ is given by the Equation 3.3, and $SP\sigma$ ids given bay the followin equation.

$$SP\sigma = \begin{cases} SP\sigma_{low} \\ SP\sigma_{high} \end{cases} \tag{3.8}$$

The results of model 2 show a lower fit (DIC= 12039.17) than model 1. It was therefore possible to find a model that could explain the stable uncertainty case but does not apply to the volatility condition, suggesting that the model may need to be made more complex by adding/fitting new parameters.

3.2.2 Neurobiological Results

3.2.3 The parietal cortex participate of the modulation of learning rate

Based on the behavioral results obtained and our hypothesis, we focused on analyzing the neurobiological activity associated with the process of learning rate updating in the conditions proposed in the task in the

period of decision making and feedback. The model considers:

BOLD signal=Stable Uncertain Low+Stable Uncertain High+Uncertain Volatile Low+Uncertain Volatile High

The presence of uncertainty was considered as a dummy. From this analysis we did not obtain results neither for the decision making period nor the feedback, so we weighed the parameters by the learning rate of each trial in each subject in each condition. The calculation of alpha was done as follows:

$$\alpha_t = \frac{Prediction_{(i+1)} - Prediction_{(i))}}{PE_{(i)}}$$

The BOLD signal analysis showed that for the contrast between High Volatile Uncertainty and Low Volatile Uncertainty in the alpha-weighted feedback period there is an increase of activity in the Parietal cortex, specifically in the supramarginal gyrus.

3.3 Discussion

We investigated decision making in the context of stable uncertainty and volatility with the aim of analyzing the neurobiological and behavioral activity associated with uncertainty computation in tasks involving learning. Participants were required to make a decision and observe feedback to construct the probabilistic distribution in each gambling condition. Our findings show that there is a statistically significant difference in the rate of learning that is modulated in the decision-making process in unstable contexts. In addition, an increase in BOLD signal was observed in the parietal cortex during feedback in the high volatility condition, this indicates that PC might be involved in the learning rate adjustment process .

Our findings show that the learning rate in volatile contexts is higher than in stable contexts, this is consistent with previous literature (Diederen et al., 2016). Evidence shows that the parietal cortex is

involved in processing uncertainty in contexts of ambiguity (?, ?), however studies have not revealed its involvement in a major role in the processing of the learning rate update.

From the data obtained, we can say that it is possible to estimate that the parietal cortex is involved in modulating the rate of learning in volatile contexts.

3.4 Material and Method

3.4.1 Participants

Forty-eight healthy, Spanish-speaking subjects, aged 18-35 years, participated in the experimental protocol approved by the Ethics Committee of the Universidad del Desarrollo, Chile. Thirty subjects participated in the fMRI and behavioural session, eighteen participated only in the behavioural test at the piloting stage. All participants had normal or corrected-to-normal vision, no colour vision problems, no history of neurological disease, and no current psychiatric diagnosis or psychotropic prescriptions. All participants gave informed consent. All experiments were performed at the Advanced Quantitative Imaging Unit of the Clínica Alemana de Santiago.

3.4.2 Task

In the fMRI experimental session, participants solved an average of 118 trials divided into 8 conditions: 4-7 trials for the stable high, low, false and noisy uncertainty condition, 8-12 trials for the volatility condition with high and low uncertainty.

In this decision making task in the context of stable uncertainty and volatility (DMUV), participants have to predict where they think an arrow shot by an archer whose target is unknown will land. In the first instance a screen is presented with a cue indicating in which condition they are making their prediction. The cue is an image indicating the context of the task and the distance of the archer from the bow. The context is given by the number of targets presented in the cue. If 1 bow is presented, the participant must make his/her decision in the context of stable uncertainty, i.e. the archer will always aim at the same target. On the contrary, if 2 arcs are presented, the archer might decide to change his target once during the task, thus it is a context of volatility. Once the target change occurs, the target remains stable. The distance to

the archer is represented by an arrow at the bottom of the cue. Either a short arrow or a long arrow can be presented to indicate whether the archer is close (short arrow) or far away from his target (long arrow). The distance of the archer represents the uncertainty level of the task, i.e. if the archer is far away from the target the prediction is made in a high uncertainty condition (sigma +/- 7 units). Conversely, if the archer is close to the target, the decision making occurs in a context of low uncertainty (sigma +/- 3 units). The following screen shows a red bar representing the wall at which the archer shoots the arrows. This red bar is divided into 20 parts or 20 options that players can choose to make their prediction of where they estimate the arrow will land. The red bar contains a white bar that indicates the position on the wall that is possible to choose. The white bar is randomly placed on each trial. Once the player has made their prediction, a screen appears showing feedback on the decision. Here the wall contains the white bar representing the subject's decision, a purple bar representing the correct answer or where the arrow landed and the distance between the prediction and the correct answer is marked with yellow to represent the magnitude of the error in the prediction. Participants are told that the more accurate the prediction, the higher is the reccompense .

3.4.3 Anatomical Data

All participants underwent a T1- and T2-weighted MPRAGE anatomical scan on a Siemens Skyra 3T (Siemens AG, Erlangen, Germany) in the fMRI experiment. The anatomical volume consisted of 160 sagittal slices of an isotropic voxel (1x1x1 mm), covering the whole brain. The scalp and cerebral cortex surfaces were extracted from the anatomical T1/ T2-corrected MRI using the pipeline available from the Human Connectome Project.

-	Median	Mean	psrf
$mu.\alpha_{\mu}$	0.54706	0.5475	1.0058
$mu.\alpha_{\sigma}$	0.25724	0.26008	1.5457
$deviance$	13704	13704	1.0042

Table 3.1: **Behavioral results of Model 1: α_{μ} and 1 α_{σ} for all conditions.** Result obtained considering all conditions of the DMUV task. DIC= 13767.01 , n=48.

-	Median	Mean	psrf
$mu.\alpha_{\mu}$	0.52664	0.52514	1.5023
$mu.\alpha_{\sigma}$	0.40929	0.41331	1.0986
$deviance$	1081.8	1082.2	1.0844

Table 3.2: **Behavioral results of Model 1: α_{μ} and 1 α_{σ} of low stable uncertain condition.** DIC= 1168.151 , n=48.

-	Median	Mean	psrf
$mu.\alpha_{\mu}$	0.48491	0.49156	367.18
$mu.\alpha_{\sigma}$	0.48361	0.49215	114.11
$deviance$	1518.9	1509.6	8.5298

Table 3.3: **Behavioral results of Model 1: α_{μ} and 1 α_{σ} of low uncertain volatile condition.** DIC= 3936.716 , n=48.

-	Median	Mean	psrf
$mu.\alpha_{\mu}$	0.5334	0.53376	1.0008
$mu.\alpha_{\sigma high}$	1.8046	1.8057	0.99967
$mu.\alpha_{\sigma low}$	1.3286	1.3276	1.0635
$deviance$	11949	11949	1.0001

Table 3.4: **Behavioral results of Model 2: α_{μ} and 2 α_{σ} for all condition.** DIC= 12039.17 , n=48.

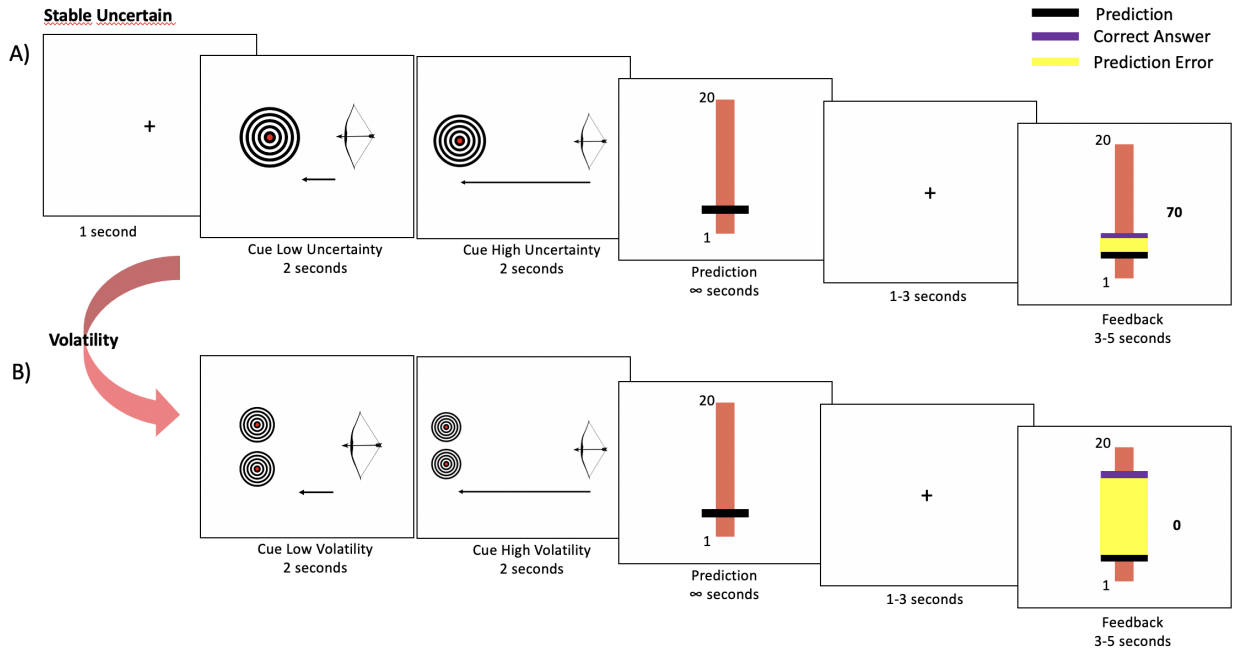

Figure 3.1: **Decision-Making under Uncertainty and Volatility task (DMUV). A.** Stable Uncertainty Condition **B.**Volatile Condition

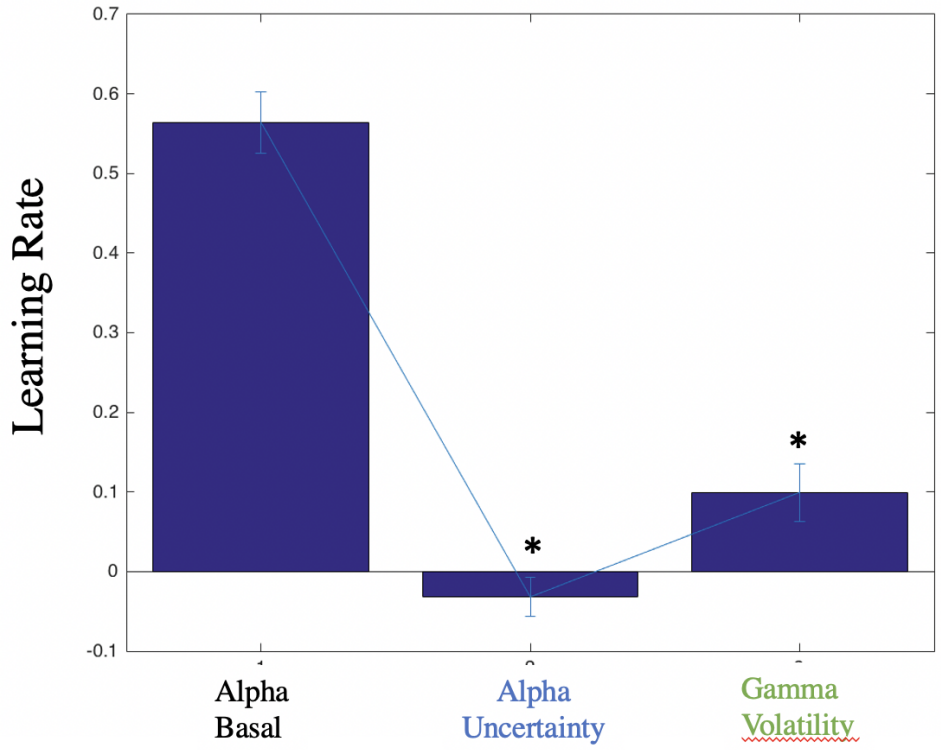

Figure 3.2: **Resultados conductuales de α_U and α_V.** Learning rate decrease in Stable Uncertainty condition (mean alpha -0.0319, p value 0.0183) and the Learning rate increase in Volatility condition (mean gamma 0.0994, p value 0.0271), n=48 subjects.

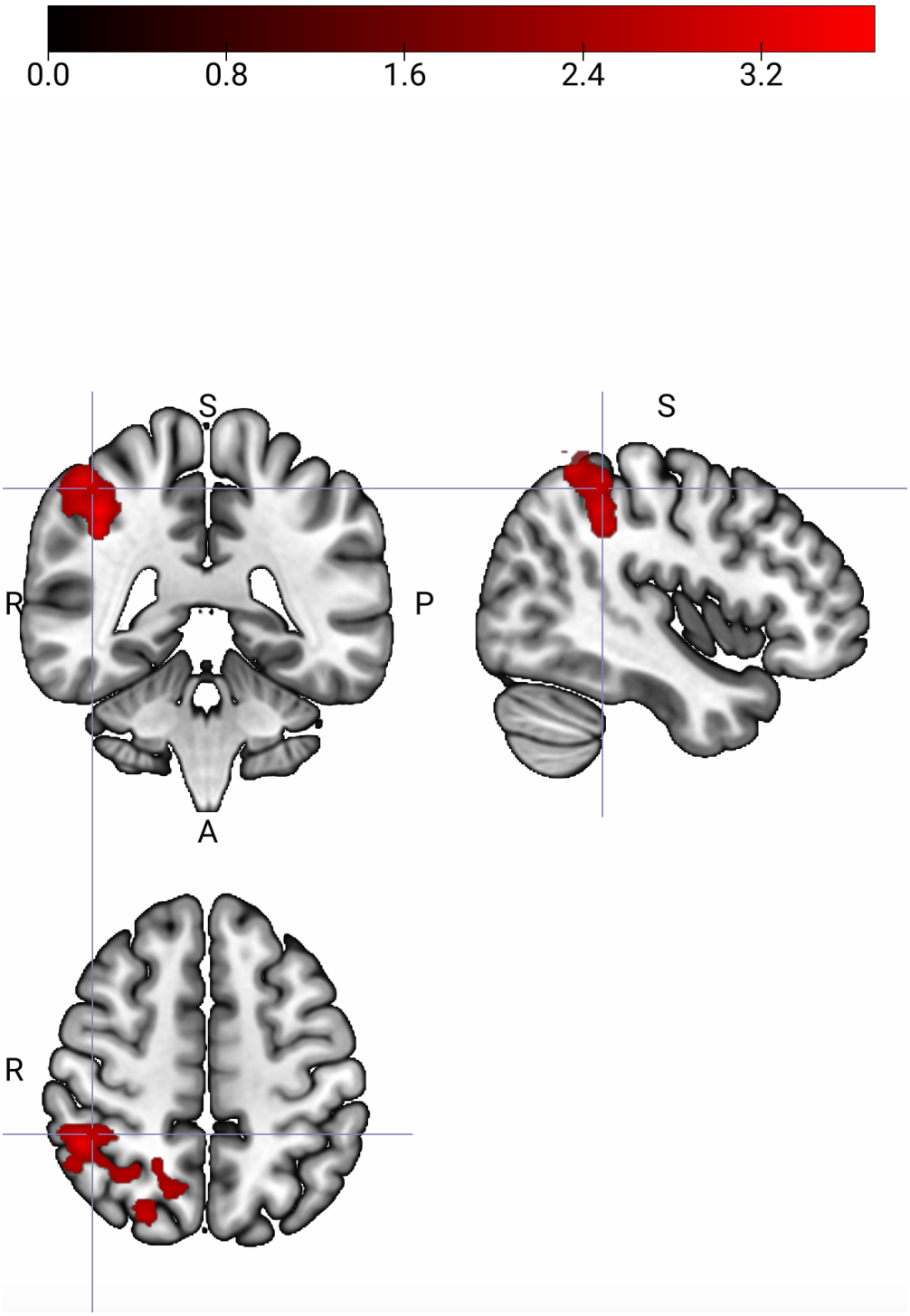

Figure 3.3: **Neurobiological activity associated to α_t during feedback.** Brain Activity during feedback in High Volatility context (z threshold = 2.3, corrected cluster p < 0.01)

References

Angela, J. Y., & Dayan, P. (2005). Uncertainty, neuromodulation, and attention. *Neuron*, *46*(4), 681–692.

Aston-Jones, G., & Cohen, J. D. (2005). Adaptive gain and the role of the locus coeruleus–norepinephrine system in optimal performance. *Journal of Comparative Neurology*, *493*(1), 99–110.

Bernat, E. M., Nelson, L. D., Holroyd, C. B., Gehring, W. J., & Patrick, C. J. (2008). Separating cognitive processes with principal components analysis of eeg time-frequency distributions. In *Advanced signal processing algorithms, architectures, and implementations xviii* (Vol. 7074, pp. 240–249).

Billeke, P., Ossandon, T., Perrone-Bertolotti, M., Kahane, P., Bastin, J., Jerbi, K., … Fuentealba, P. (2020). Human anterior insula encodes performance feedback and relays prediction error to the medial prefrontal cortex. *Cerebral Cortex*, *30*(7), 4011–4025.

Bland, A. R., et al. (2012). Different varieties of uncertainty in human decision-making. *Frontiers in neuroscience*, *6*, 85.

Boorman, E. D., Rushworth, M. F., & Behrens, T. E. (2013). Ventromedial prefrontal and anterior cingulate cortex adopt choice and default reference frames during sequential multi-alternative choice. *Journal of Neuroscience*, *33*(6), 2242–2253.

Cavanagh, J. F., Cohen, M. X., & Allen, J. J. (2009). Prelude to and resolution of an error: Eeg phase synchrony reveals cognitive control dynamics during action monitoring. *Journal of Neuroscience*, *29*(1), 98–105.

Clark, A. (2013). Whatever next? predictive brains, situated agents, and the future of cognitive science. *Behavioral and brain sciences*, *36*(3), 181–204.

Cohen, M. X., & Ranganath, C. (2007). Reinforcement learning signals predict future decisions. *Journal of Neuroscience*, *27*(2), 371–378.

D'Ardenne, K., McClure, S. M., Nystrom, L. E., & Cohen, J. D. (2008). Bold responses reflecting dopaminergic signals in the human ventral tegmental area. *Science*, *319*(5867), 1264–1267.

Dayan, P., & Jyu, A. (2003). Uncertainty and learning. *IETE Journal of Research*, *49*(2-3), 171–181.

Dayan, P., & Yu, A. J. (2006). Phasic norepinephrine: a neural interrupt signal for unexpected events. *Network: Computation in Neural Systems*, *17*(4), 335–350.

Diederen, K. M., Spencer, T., Vestergaard, M. D., Fletcher, P. C., & Schultz, W. (2016). Adaptive prediction error coding in the human midbrain and striatum facilitates behavioral adaptation and learning efficiency. *Neuron*, *90*(5), 1127–1138.

Domenech, P., Redouté, J., Koechlin, E., & Dreher, J.-C. (2018). The neuro-computational architecture of value-based selection in the human brain. *Cerebral Cortex*, *28*(2), 585–601.

Doya, K. (2008). Modulators of decision making. *Nature neuroscience*, *11*(4), 410–416.

Falkenstein, M. (1990). Effects of errors in choice reaction tasks on the erp under focused and divided attention. *Psychophysiological brain research*.

Friston, K. (2012). The history of the future of the bayesian brain. *NeuroImage*, *62*(2), 1230–1233.

Gehring, W. J., Coles, M. G., Meyer, D. E., & Donchin, E. (1990). The error-related negativity: an event-related brain potential accompanying errors. *Psychophysiology*, *27*(4), S34.

Glimcher, P. W., & Fehr, E. (2013). *Neuroeconomics: Decision making and the brain*. Academic Press.

Gueguen, M., Lopez-Persem, A., Billeke, P., Lachaux, J.-P., Rheims, S., Kahane, P., … Bastin, J. (2021). Anatomical dissociation of intracerebral signals for reward and punishment prediction errors in humans. *Nature communications*, *12*(1), 1–12.

Huettel, S. A., Song, A. W., & McCarthy, G. (2005). Decisions under uncertainty: probabilistic context influences activation of prefrontal and parietal cortices. *Journal of Neuroscience*, *25*(13), 3304–3311.

Kable, J. W., & Glimcher, P. W. (2009). The neurobiology of decision: consensus and controversy. *Neuron*, *63*(6), 733–745.

Kahneman, D., & Tversky, A. (2013). Prospect theory: An analysis of decision under risk. In *Handbook of the fundamentals of financial decision making: Part i* (pp. 99–127). World Scientific.

Knill, D. C., & Pouget, A. (2004). The bayesian brain: the role of uncertainty in neural coding and computation. *TRENDS in Neurosciences*, *27*(12), 712–719.

Knutson, B., & Wimmer, G. E. (2007). Splitting the difference: how does the brain code reward episodes? *Annals of the New York Academy of Sciences*, *1104*(1), 54–69.

Ma, W. J., & Jazayeri, M. (2014). Neural coding of uncertainty and probability. *Annual review of neuroscience*, *37*, 205–220.

Marco-Pallares, J., Cucurell, D., Cunillera, T., García, R., Andrés-Pueyo, A., Münte, T. F., & Rodríguez-Fornells, A. (2008). Human oscillatory activity associated to reward processing in a gambling task. *Neuropsychologia*, *46*(1), 241–248.

Miltner, W. H., Braun, C. H., & Coles, M. G. (1997). Event-related brain potentials following incorrect feedback in a time-estimation task: evidence for a "generic" neural system for error detection. *Journal of cognitive neuroscience*, *9*(6), 788–798.

Montague, P. R., Dayan, P., & Sejnowski, T. J. (1996). A framework for mesencephalic dopamine systems based on predictive hebbian learning. *Journal of neuroscience*, *16*(5), 1936–1947.

Polanía, R., Krajbich, I., Grueschow, M., & Ruff, C. C. (2014). Neural oscillations and synchronization differentially support evidence accumulation in perceptual and value-based decision making. *Neuron*, *82*(3), 709–720.

Polezzi, D., Sartori, G., Rumiati, R., Vidotto, G., & Daum, I. (2010). Brain correlates of risky decision-making. *Neuroimage*, *49*(2), 1886–1894.

Quirk, G. J., & Mueller, D. (2008). Neural mechanisms of extinction learning and retrieval. *Neuropsychopharmacology*, *33*(1), 56–72.

Rangel, A., Camerer, C., & Montague, P. R. (2008). A framework for studying the neurobiology of value-based decision making. *Nature reviews neuroscience*, *9*(7), 545–556.

Sales, A. C., Friston, K. J., Jones, M. W., Pickering, A. E., & Moran, R. J. (2019). Locus coeruleus tracking of prediction errors optimises cognitive flexibility: An active inference model. *PLoS computational biology*, *15*(1), e1006267.

Schultz, W. (2016). Dopamine reward prediction-error signalling: a two-component response.

Nature reviews neuroscience, *17*(3), 183–195.

Schultz, W., Apicella, P., & Ljungberg, T. (1993). Responses of monkey dopamine neurons to reward and conditioned stimuli during successive steps of learning a delayed response task. *Journal of neuroscience*, *13*(3), 900–913.

Sutton, R. S., & Barto, A. G. (2018). *Reinforcement learning: An introduction*. MIT press.

Trujillo, L. T., & Allen, J. J. (2007). Theta eeg dynamics of the error-related negativity. *Clinical Neurophysiology*, *118*(3), 645–668.

Yeung, N., & Sanfey, A. G. (2004). Independent coding of reward magnitude and valence in the human brain. *Journal of Neuroscience*, *24*(28), 6258–6264.

Zhang, S., Hu, S., Chao, H. H., & Li, C.-S. R. (2016). Resting-state functional connectivity of the locus coeruleus in humans: in comparison with the ventral tegmental area/substantia nigra pars compacta and the effects of age. *Cerebral Cortex*, *26*(8), 3413–3427.